2019

Novel DNA Origami Based Lateral Flow Assay Development

Adrienne Walker

NOVEL DNA ORIGAMI BASED LATERAL FLOW ASSAY DEVELOPMENT

A thesis submitted to
the Graduate College of
Marshall University
In partial fulfillment of
the requirements for the degree of
Master of Science
In
Chemistry
by
Adrienne Walker
Approved by
Dr. Michael Norton, Committee Chairperson
Dr. Scott Day
Dr. Bin Wang

Marshall University
May 2019

APPROVAL OF THESIS

We, the faculty supervising the work of Adrienne Walker, affirm that the thesis, *Novel DNA Origami Based Lateral Flow Assay Development*, meets the high academic standards for original scholarship and creative work established by the Department of Chemistry and the Marshall University Graduate School. This work also conforms to the editorial standards of our discipline and the Graduate College of Marshall University. With our signatures, we approve the manuscript for publication.

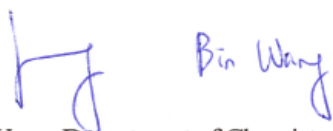|		
Dr. Michael Norton, Department of Chemistry	Committee Chairperson	11/22/19 Date
Dr. Scott Day, Department of Chemistry	Committee Member	1/23/2019 Date
Dr. Bin Wang, Department of Chemistry	Committee Member	1/23/2019 Date

ACKNOWLEDGEMENTS

TABLE OF CONTENTS

LIST OF TABLES

LIST OF FIGURES

ABSTRACT

Lateral flow assays (LFA) are used for point-of-care qualitative diagnostics of an analyte of interest, often in non-laboratory environments. Traditionally, the format of a lateral flow assay is to utilize immobilized antibodies on a membrane as the capture probe in conjunction with a reporting immunological recognition system for an analyte captured between them in a sandwich format. However, there are several shortcomings of antibodies which recommend their replacement with other recognition elements, if possible. The research described in this thesis was directed toward using several of the inherent properties of DNA based Origami nanostructures to enable the construction of DNA based LFAs. DNA Origami constructs consist of a scaffold strand, staple strands (to direct for the folding of helices to conform to the specification of the design) and modified staple strands. Programmable functionalities include specific DNA structures, nanoparticles, proteins and a wide range of chemical modifications. The three types of modifications which were investigated as potential analyte binding mechanisms included: 1) ssDNA hybridization, 2) Tris-Nitrilotriacetic Acid (Tris-NTA)-his tagged protein binding and 3) binding to Thrombin through aptamers. The capture probe of the lateral flow assay was immobilized on an analytical Nitrocellulose membrane. The mobile reporting probe DNA Origami construct was modified to enable binding of Gold nanoparticles which provide a mechanism for development of a visible, characteristic red report line at the test site, indicative of a positive test result.

CHAPTER 1: STUDY OVERVIEW

1.1 MOTIVATION OF STUDY

Lateral flow immunological assays have been used for many years in lab settings and in the field for point-of-care detection of specific analytes.[1] Conventionally, analyte-specific antibodies are used to detect the analyte in question in these assays. A few drawbacks to using antibodies for LFAs include: 1) the high cost of creating antibodies against a single epitope of an antigen or analyte, 2) the long process to develop specific antibodies and 3) the risk of loss of the clone line. Due to these disadvantages, other types of capture and reporting probes have been proposed for use in LFAs. DNA Origami provides a stable self-assembling structure which can be modified with multiple different functionalities. The programmability and ability to orient molecules allows for design and creation of antibody-like DNA structures, with the capture and reporting capabilities inherent to components of traditional assays. To our knowledge, a paper-based assay using DNA Origami as the probes has not been studied previously.

CHAPTER 2: REVIEW OF LATERAL FLOW TECHNOLOGY AND PROPOSED DNA ORIGAMI LFA DESIGNS

2.1 INTRODUCTION TO LATERAL FLOW ASSAYS

Lateral flow assays are used for qualitative and semiquantitative analyses of certain pathogens, drugs, hormones and metabolites in non-laboratory environments.[1] The most notable lateral flow assays are used to detect human chorionic gonadotropin (hCG), a chemical marker associated with pregnancy.[2] Fields in which LFAs have been applied include biomedical, veterinary, food safety and environmental detection of pathogens. The tests are user-friendly since the user needs little to no laboratory experience, the results are available in a short time and tests are relatively inexpensive. The usability and applications of rapid response detection elements motivated further studies into these particular assays.

There are many different designs for LFAs prominently including competitive and sandwich assays which use either antibodies or DNA/RNA.[1] Competitive assays are used when
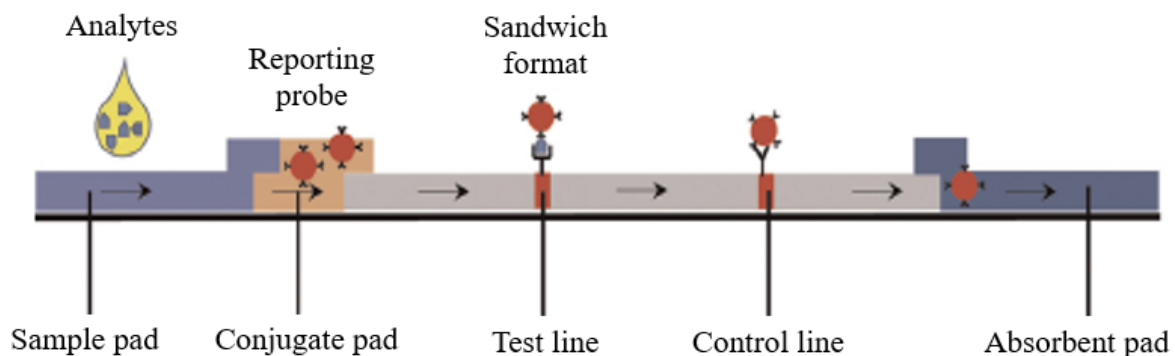
Figure 1 – Schematic representation of a lateral-flow assay in sandwich format.[3]

testing for small molecules against a single antigen.[1] Here we focus on sandwich assays. Sandwich style assays are used for larger molecules with two possible reactive antigenic sites (Figure 1). An assortment of ligands can be bound to a detectable support species, which can

then test for an analyte specific to that ligand. These assays are typically designed with signaling elements, such that the reporting line appears if the target species is present.

In this research, different designs for rapid lateral-flow based tests, using DNA Origami
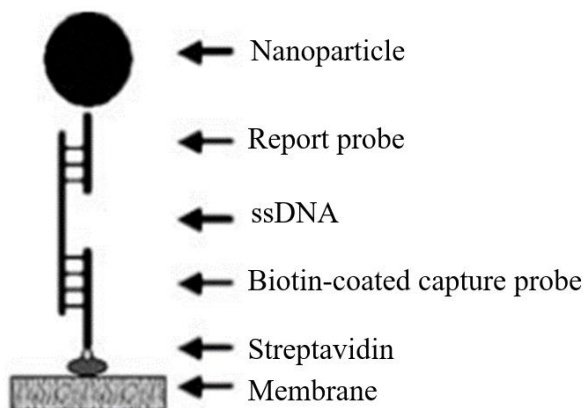
Figure 2 – Schematic representation of a nucleic acid LFA. A nucleic acid lateral flow assay depicted using functionalized nanoparticles as the reporting probe and a biotinylated capture probe to then hybridize with DNA to report a signal if analyte is present.[1]

as probes in the assay, have been developed. Three designs for lateral flow tests proposed and developed here use sandwich hybridization to detect sequences of DNA, immobilization of a His-tagged protein and capture of human thrombin protein. The design used in this research most closely resembles that of a nucleic acid lateral flow test format: nanoparticle-labelled mobile reporter probe and biotin-labelled immobilized capture probe uses DNA hybridization to yield a signal (Figure 2). In the review of paper-based lateral flow assays by Posthuma-Trumpie et al., many researchers use sequences of nucleic acids as the detection element and AuNPs are used as the reporter element.[1] However, in our work, the developed probes were made out of dsDNA structures, more notably known as DNA Origami. The use of DNA Origami in LFAs is a novel concept and shows promise in application to point-of-care detection devices due to programmability of the DNA construct.

2.2 LATERAL FLOW ASSAY COMPONENTS

Before testing of complete LFA function could begin, many different probe options were suggested and characterized to display the efficacy of a DNA Origami based lateral flow assay. The component materials of the DNA Origami LFAs were carefully selected after review and experimentation. The components of an LFA[4] are listed below.

- Probes:
    - Immobile Capture Probe: Test line, Control line
    - Capture mechanism: DNA hybridization, Tris-Nitrilotriacetate complexation with a His-tag and DNA aptamers.
    - Mobile Reporting Probe: Reporting a signal at capture
        - Optically Visible Particles:
            - Nanoparticles or microspheres: 1/10 the pore size of the membrane so migration is possible
            - Pretreatment of membrane is necessary to minimize hindered flow of the nanoparticles and probes through the membrane

The probe components of the DNA Origami based LFAs are discussed in greater detail in the next few sections. The probe selection and design preceded the membrane component selection of the DNA Origami based LFA. Membrane selection was informed by experimentation.

- Membranes:
    - Options for membranes: Nitrocellulose (high-protein binding), Cellulose Acetate (low-protein binding) and Glass Fiber Membranes (non-protein binding)

- Conjugate Pads:

    - Pad is made of a material that can absorb a large amount of sample as well as house and release the conjugate reporting probe at a constant rate once sample is added

- Membrane Backing:

    - Strengthens the membrane and eliminates the possibility of adhesives interfering with the test

- Plastic Housing:

    - Final product is presented in housing to support the assay for storage and transport

2.3 INTRODUCTION TO PROBE DESIGN

2.3.1 DNA Origami

Rothemund, in 2006, was the first to pioneer the process of creating the folded nanostructures called DNA Origami.[5] The design of DNA Origami nanostructures allows for arrangement of modifications onto the nanostructures with extraordinary precision. The self-assembly process begins with a long ssDNA scaffold strand which often consists of circular ssM13 viral DNA to which specific complementary ssDNA staple strands are added. During an annealing process, helices are created via Watson-Crick hydrogen bonding between complementary bases in order to fold the scaffold into programmed shapes (Figure 3). These

interactions are highly specific due to the free energy of association between unique non-repeating sequences of DNA.[6]
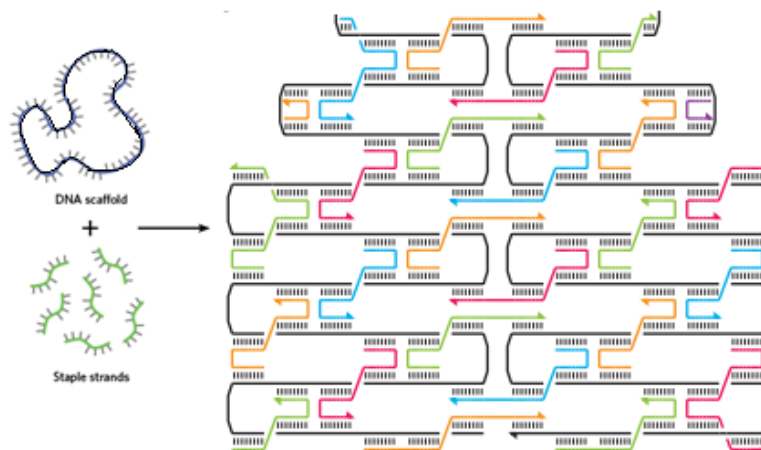
Figure 3 - Depiction of components and self-assembling DNA Origami. ssDNA viral M13 scaffold strand (blue/black) and ssDNA staple strands (multicolored) mixed together creating designs using hybridization.[5]

For the purposes of this research, around two hundred 32 base-average length non-repeating sequences of ssDNA are used as staple strands which hybridize with the M13 scaffold strand to create a cross-shaped DNA Origami structure. Using this technique, identical nanoscale structures can be assembled in large quantities (trillions/ml) which have the same modifications encoded. Each individual staple strand in the construct can be used as a precise attachment point for modifications, which are either directly attached via the DNA backbone or hybridized through a complementary strand.[7-9]

DNA Origami can be used as a substrate for studying chemical reactions.[10] The structures provide an object upon which to place binding sites with nanometer precision and modifications enabling chemical processes. Many modifications are achievable using functionalized staple strands, either as a modification incorporated into the DNA backbone or extended regions of

DNA to elicit hybridization. The yield and efficiency of folding, designs and the quality of final constructs are typically analyzed using atomic force microscopy (AFM) imaging.[7] Imaging using AFM is an efficient technique due to the ability to operate under atmospheric conditions and the simple deposition process used for sample preparation.

Atomic force microscopy (AFM) and gel electrophoresis were used to characterize and verify the structure of the separately designed constructs. AFM scans a cantilever with a sharp tip over the surface of the sample, usually deposited on a prepared piece of mica which serves as an ultra-flat solid surface. The cantilever detects interaction forces between itself and the sample which include: van-der-Waals forces, electrostatic forces, capillary attractions and Pauli repulsions. Interactions result in deflections of the cantilever which provide information about sample topography. This method generates an image of the surface topography with a lateral resolution of 1-10 nm and a height resolution of 0.1 nm. The x and y axis are not as reliable as the z axis measurement of the AFM; however, if the object in question is distinguishable against a counterpart, binding confirmation can be achieved. The AFM can distinguish extremely small differences in height and this feature of the microscope can allow us to know with some certainty that the DNA Origami designs functioned as expected.

2.3.2 Modifications to DNA Origami for Development of an LFA

To further program these constructs, functionalities were bound to certain staples in the design and displayed the ability of DNA Origami to 1) precisely bind and present a protein, 2) to extend ssDNA for hybridization and 3) present gold nanoparticles on site specific locations. CO_3970 (Figure 4), the construct used in this research, is an optimized (Norton Nanolabs) permutation of Seeman's original cross shaped DNA Origami.[6] The programmed functionalities implemented for the CO_3970 construct in this research consist of 1) 6 polyA(10) and 6 polyT(10) strands on the right and left ends of the different cross constructs (capture and reporting probes indicated in Figure 5) in order to enable two separate constructs to hybridize
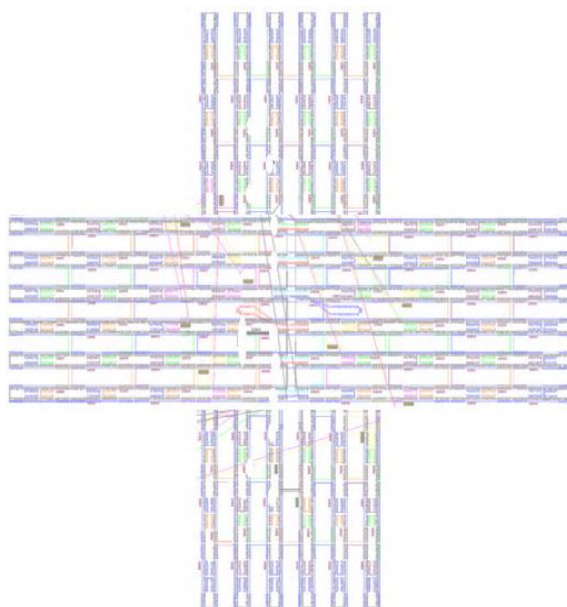
Figure 4 - CO_3970 construct. The construct which will be functionalized with specific modifications. The design is an adaptation to N. Seeman original cross DNA Origami design.[6]

with each other, creating one capture mechanism (Figure 5), 2) adding a Tris-Nitrilotriacetate (Tris-NTA) modification on the 5' end of a staple strand for Ni^{2+} complexation and subsequent binding of a His-tagged protein 3) adding the sequences for aptamers to the probes to enable a

sandwich assay and 4) decorating 3 precisely designed sites with staples extended with sequences which are complementary to the specific sequence of Thiolated ssDNA used to functionalize gold nanoparticles (Figure 5). As described in a later section, the aptamers were used in another proposed design utilizing thrombin binding aptamers. The modifications were intended to allow CO_3970 to function like the probes for use in the paper-based chromatography technique known as a lateral flow assay.
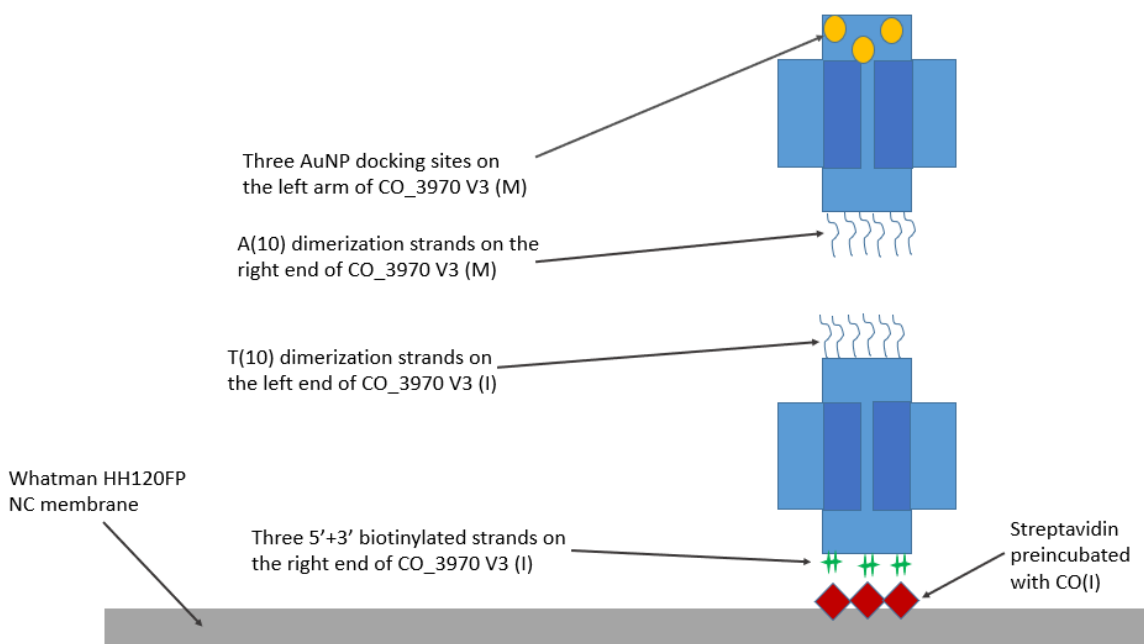
Figure 5 - Schematic representation of DNA Origami mobile and immobile probes used in ssDNA hybridization LFA. DNA Origami LFA depicting the capture and subsequent positive result when the ssDNA on the capture CO(I) probe and the mobile CO(M) reporting probe hybridizes. V3 designates the 3rd version of the constructs.

When modifications are integrated into new designs, the original unmodified staple sequences are excluded from the reaction mixture and the newly modified staple or staples are then added to the synthesis solution. To speed hybridization and increase yield, the solution containing all sequences was heated to $90^{o}C$, an appropriate DNA melting temperature, then cooled ($90^{o}C$-$20^{o}C$) to produce the functionalized constructs. Further details about the formation of these structures are provided in the procedures section. The designs are easily manipulated

and only take ~6 hours to create by using this temperature program to enable hybridization

between the M13 ssDNA scaffold and the ssDNA staple strands to occur. The easy manipulation

is key to creating variations of these structures which are advantageous in tailoring capture or

reporting probes for specific purposes.

The mobile reporting probe design has 3 red, plasmonically active (electron density

fluctuation coupling with electromagnetic radiation) gold nanoparticles bound to it to enable

visualization. The mobile reporting probe rapidly reacts with the immobilized probe at the test

line through DNA hybridization between these constructs (Figure 5). Binding is verified by the

observation of a visible red line.

2.3.2a ssDNA Hybridization

The ssDNA hybridization reaction, using complementary sequences, has been

extensively studied.[9] The ability for ssDNA to hybridize spontaneously with its complement is

Right arm of CO_3970: with polyA(10) strands integrated into the mobile reporting probe.

Left arm of CO_3970: with polyT(10) strands integrated into the immobilized capture probe.
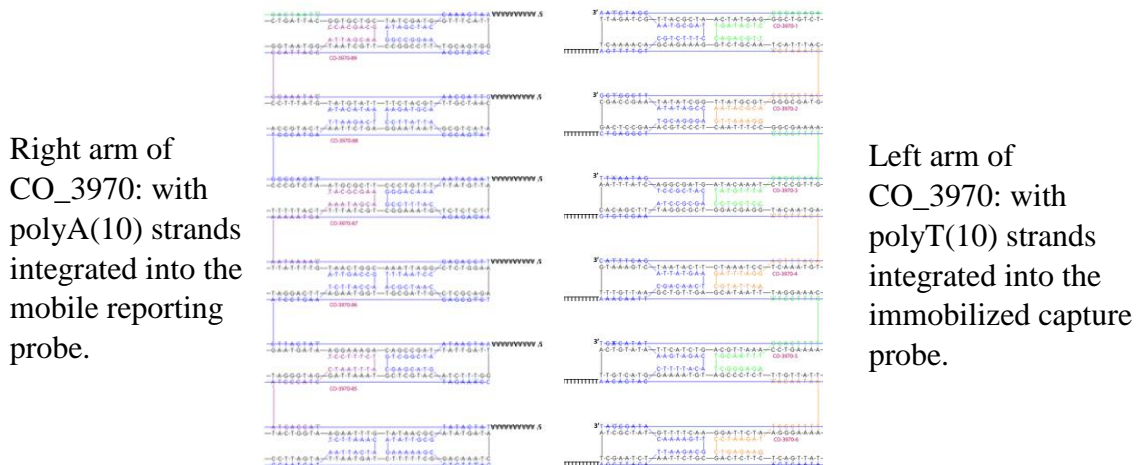
Figure 6 - The polyA and polyT modified ssDNA staples integrated into the right and left arm of the CO_3970 mobile and immobile construct. The polyA modified strands are integrated into the mobile reporter probe of the LFA and the polyT modified strands are integrated into the probe which will be immobilized onto the analytical membrane.

due to the free energy of binding for the bases pairing the ssDNA strands. Selected staple strands in our construct were designed to have either 10 Thymine or 10 Adenine bases protruding from one of the arms of the CO_3970 in order to test concept design (Figure 6). These 2 variations are separate constructs designed with the capture mechanism of a sandwich lateral flow assay in mind and were designated the mobile and immobile probes. Studies suggest that the correct contact of just 6 complementary base-pairs display a free energy of binding of ~8 to 14 kcal mol^{-1}.[12] The rate of spontaneous binding of these complementary ssDNA sequences allows for creation of a rapidly capturable reporter Origami construct. The reporter construct has AuNPs bound to it to enable visualization. The ssDNA hybridization assay design imitates previous work with RNA and DNA targets for LFAs and the DNA Origami probes could be integrated with target specific sequences for recognition of viral RNA and DNA targets.[13-16]

2.3.2b Tris-Nitrilotriacetic Acid

The Tris-Nitrilotriacetate (Tris-NTA) functionalized ssDNA (Figure 7) programmed into the Origami, will, in the presence of certain transition metal ions, allow for reversible

TrisNTA-modified DNA
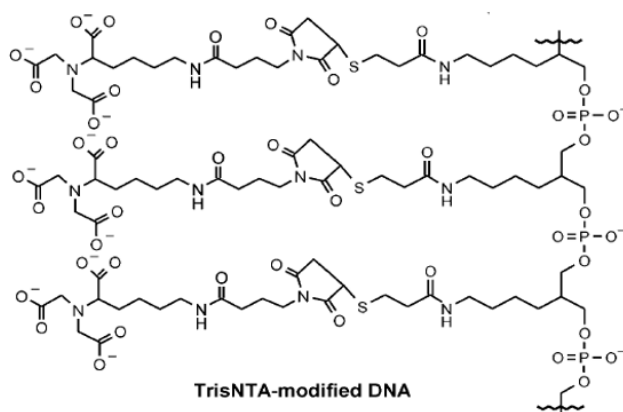
Figure 7 - Tris-NTA modified DNA. Tris-NTA ssDNA modification which was added to the 5' end of ssDNA staple.[17]

immobilization of a His-tagged fluorescent protein, or any 6 His-tagged protein, onto the specific site of the construct.[17] The 6-coordinate system of Ni^{2+} ions allows for covalent coordinate bonding with the tetra-coordinating NTA molecule which acts as a multivalent chelator. Once 3 Ni^{2+} ions are bound to the three consecutive NTA molecules on the ssDNA, two coordination sites on each of the ions area are left unoccupied. Two Histidine residues then chelate each Ni^{2+} ion, providing a mechanism for immobilization of 6-His-tagged proteins (Figure 8 and 9).[18] This multivalent chelation of a His-tagged protein enables quantitative studies of binding interactions to solid surfaces such as DNA Origami.[19] In some cases the interaction does not compromise the protein's inherent function.[18]

The metal chelating reaction of the Tris-NTA is similar to the reactions used in some chromatography techniques for Histidine tagged protein purification, in which chelated metal ions are added in order to elute off and purify multi-protein solutions.[18,20] This protein
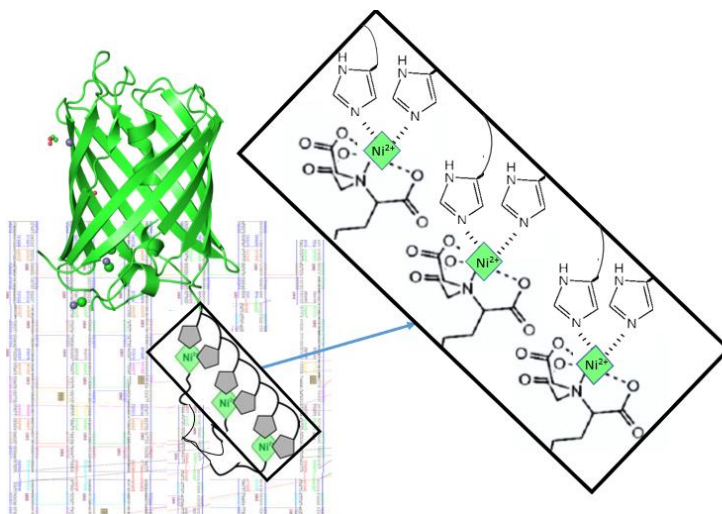
Figure 8 – Schematic representation of a Tris-NTA modified ssDNA staple integrated into the left arm of the CO_3970 construct. Ni^{2+} ions are chelated both by the NTA molecules incorporated into the DNA Origami and the Histidine residues of the fluorescent protein. Ni^{2+} environment reproduced from Goodman et al.[17]

purification method was the inspiration for using this NTA metal chelating reaction in a possible

design to capture His-tagged proteins with DNA Origami.[19] The purification applications of the

interaction exploit the fact that the amino acid Histidine is relatively rare in occurrence in protein

structures. The imidazole moiety of the His amino acid is the functional fragment of the structure

which displays an affinity for transition metal ion chelation. However, coordination of His

residues to the preloaded Ni(II)-NTA molecules results in a relatively low binding affinity.[21] To

counteract this low affinity, multiple nitrilotriacetic acid moieties were incorporated into the

DNA Origami in order to increase the stability of the complex.[22, 23]

The Tris-NTA ssDNA staple (Genelink) was incorporated into the design on the left arm

of the CO_3970 design. This modification on a designated staple strand (staple named CO_3970

#15) should enable binding of a fluorescent protein with a 6-Histidine tag, in the presence of
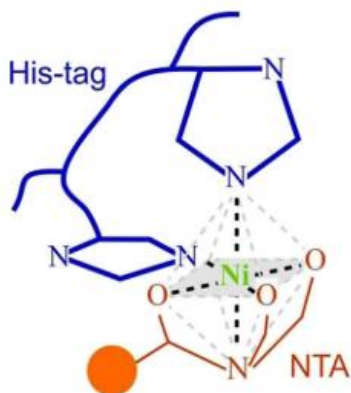
Figure 9 – Transition metal chelation by NTA and two Histidine residues. Coordinate covalent
interaction of transition metal multivalent chelator NTA, and two His residues complexed with
Ni^{2+}.[22]

$NiCl_2$, to the immobilized DNA Origami capture species of the LFA. Each Ni^{2+} ion displays an

octahedral coordination chemistry and is chelated by two Histidine residues and the tetra-

coordinating NTA ligand. mCherry fluorescent protein was selected over other fluorescent

proteins due to the compatibility of the protein's excitation wavelength (587 nm), emission

wavelength (610 nm) with the current configuration of imaging systems in the MBIC (Molecular

and Biological Imaging Center – Marshall University) and the protein's inherent photostability. The reporting function of the sandwich-style lateral flow assay would consist of the inherent fluorescence of the captured mCherry or a labeled antibody against mCherry. If the protein is used as the reporting agent then the assay will detect whether the Ni^{2+} ions, used as the analyte in the assay, were successfully sandwiched between the Tris-NTA moiety and the fluorescent protein's His-tag.

2.3.2c Thrombin Binding Aptamers

Aptamers are short single-stranded DNA or RNA molecules which form into three-dimensional structures and bind with target analytes, in a manner similar to antibodies.[24] A combinatorial DNA library is created for the selection process which has the acronym SELEX for Systematic Evolution of Ligands Exponential Enrichment.[25] A sandwich style format assay of thrombin has been developed by using two separate, different thrombin aptamers that are directed towards different epitopes. Design of an aptamer-based LFA using these thrombin aptamers has been previously reported.[3] However, none of the prior work involved using DNA Origami as the solid framework for probes.
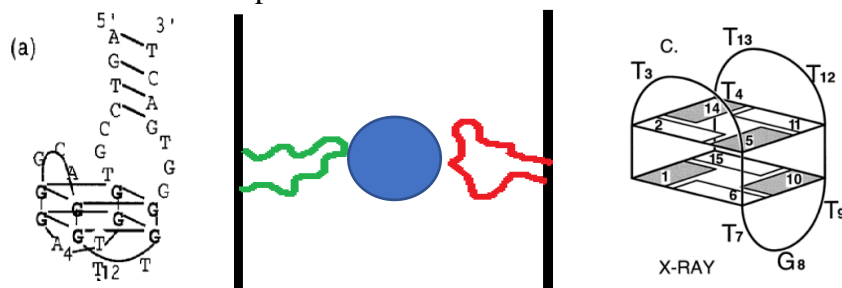
Figure 10 - Schematic of thrombin-binding aptamers bound to mobile and immobile probes with thrombin sandwiched between the probes. Thrombin binding aptamers 29 and 15 (naming refers to number of bases in the aptamer sequence). These aptamers were incorporated into the CO_3970 design and two separate designs corresponding to the immobile (TBA29) and reporting probe (TBA15) were formed. Structures are from reference 26.

The use of Thrombin binding aptamers within or extending from DNA Origami or similar nanostructures has been studied by Yan, among others.[26-30] Two different Thrombin binding aptamers were chosen to simulate the antibodies of a sandwich-style LFA (Figure 10). These aptamers were named TBA15 and TBA29 corresponding to the number of DNA bases constituting eacn aptamer. The apparent K_D values for the bivalent binding of thrombin to these two aptamers separated by a distance of 5.3 nm is 10 nM.[26]

2.3.2d Gold Nanoparticles

Gold nanoparticles were first functionalized with DNA by Mirkin and Alivisatos in 1996.[31,32] Using thiol chemistry as the particle-molecule linker, the thiolated ssDNA strands covalently bond to the gold atoms to form modified particles. ssDNA can be used to functionalize and organize metal nanoparticles onto solid supports, which unlocks new potential uses of the plasmonic and electronic properties of metal nanoparticles at the nanoscale.[33] The electron density of metal nanoparticles is susceptible to polarization induced by the electric field of incident light and the localized surface plasmon resonance (LSPR) allows these particles to become readily visible at relatively low surface densities.[34] Properties of AuNPs make them a great candidate for visualization because of their absorption of photons at 520 nm wavelength and high reflectivity of light at the near 600-700 nm range which allows, at sufficient quantities, visualization by the naked-eye.

Organizing and patterning AuNPs onto DNA Origami has been an interest of

nanotechnology research for uses in spectroscopy and microscopy due to the various optical

properties of AuNPs. Precise binding of AuNPs, selectively functionalized with ssDNA, to DNA

Origami nanostructures has been achieved within the last decade.[33-36] These programmed

structures have been put to use as a functional, AuNanorod-decorated DNA Origami Tripod

among many other things.[36] However, in this research, these structures are put to a practical use

in the creation of an LFA.
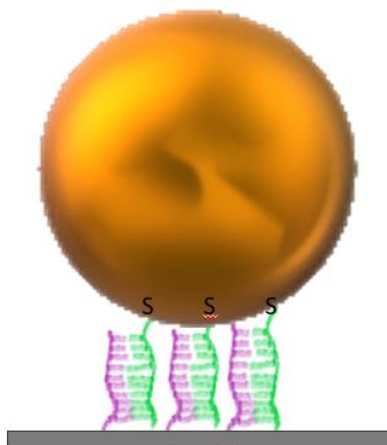
Figure 11 – Schematic of functionalized AuNP bound to complementary sequences. The 5 nm
AuNPs are functionalized with thiolated ssDNA oligonucleotides. These sequences are chosen to
be complementary to sequences extended from three staples in the DNA Origami construct
(depicted as grey bar). The hybridization of these two species can serve as a structured solid-state
probe which, in sufficient quantities, are visible when used in an LFA.

The mobile reporting probe construct design involves extending the sequence of nine

staples, such that the extended sequences are complementary to the ssDNA sequences

functionalized onto the gold nanoparticles (Figure 11). The functionalized AuNPs will then

hybridize with the staples modified with complementary strands which extend from the arm of

the DNA Origami mobile reporting probe. Three clusters of binding sites, each consisting of 3

docking strands were designed to bind a total of three AuNPs (Figure 12). These sites were

designed to be isolated geometrically in order to avoid bridging of sites by single particles. The

design concept used in spacing these sites was also useful for analysis using spectroscopic monitoring and AFM imaging. The AuNPs were functionalized with thiolated oligonucleotides which were complementary to the extended sequences on the CO_3970 design.[37-39] The gold nanoparticles were added to the construct to produce, at certain quantities, a visible indicator for successful binding at the test line. As hybridization occurs the red color characteristic of 5nm colloidal AuNPs, due to their light reflecting plasmonic properties, will appear at the test line location.
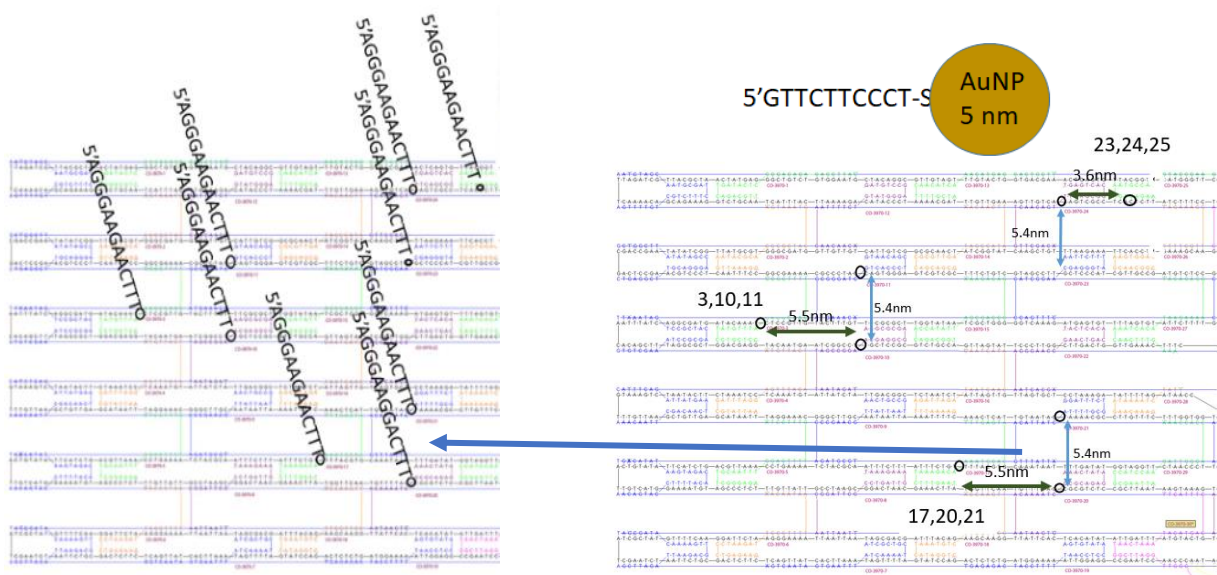
Figure 12 - Design of the AuNPs decorating the mobile reporting probe. The left arm of the CO_3970 with three 5 nm AuNP docking sites. Each of these sites are designed to allow three docking strands to bind each AuNP. The dimensions between each docking strand were measured to ensure that each site would be compatible with binding a 5 nm AuNP to the site on the Origami. The docking strand sequences are extended from the original staples of 3, 10, 11, 17, 20, 21, 23, 24 and 25 and designed to be complementary to the ssDNA used to functionalize the AuNPs[38,39].

CHAPTER 3: MATERIALS, METHODS AND PROTOCOL DEVELOPMENT FOR A DNA ORIGAMI BASED LATERAL FLOW ASSAY

3.1 AFM ANALYSIS

AFM imaging has been widely used to analyze DNA Origami because of the ability to be operated under atmospheric conditions and because the requirements for sample preparation are minimal.[7] The AFM imaging studies were performed using a Bruker Multimode 8 and Nanoscope VI controller (Billerica, MA, USA) in the setting "SCANASYST-AIR" mode, which uses off resonance tapping of the cantilever at 2000Hz. Cantilevers used in this research on the device, regularly called "tips," consist of silicon nitride with a spring constant of 0.4 N/m. Imaging parameters, such as size of scan (nm-μm) and samples per line, can be varied depending on the sample being imaged. Samples are usually imaged on mica. The Nanoscope Analysis software from Bruker was used to analyze the images to determine whether the correct site-specific binding occurred, for example DNA hybridization, binding a His-tagged protein or the binding of multiple AuNPs. The fluorescent protein and AuNPs have much different z-axis or height values. The fluorescent protein is ~2 nm in height[11] and the AuNP used in this design is 5-6 nm in height.

3.1.1 Preparation of Mica for Imaging

The mica sheet used for deposition was prepared by first obtaining a metal disc to act as a solid surface to immobilize a thin mica sheet upon. A piece of double-sided black conductive tape was adhered to the center of the metal disc. The mica slice (SPI supplies – 9.5 mm diameter) was pre-cut to fit and placed on the double-sided tape to provide a stable surface to support the

Figure 13 - Mica disc for AFM imaging. Prepared mica slip used for sample deposition and visualization using AFM.

mica (Figure 13). A fresh mica surface can then be prepared by using scotch tape to peel off the top layer of the mica. Once a fresh, clean, smooth layer of mica is presented after this peel, it is ready for dosing with a sample. The sample is deposited onto the mica surface (up to 15 µl of sample can fit on the surface). The time of incubation after deposition can be varied based on the sample's DNA concentration or different aspects of the composition of the sample. However, if depositing 5-10 µl of 1 nM DNA Origami in 1xTAE buffer with 12.5 mM $MgCl_2$, which represents standard conditions for DNA Origami, then 1-2 minutes of incubation time will suffice. Once the allotted deposition time is reached, the sample is then rinsed with minimal MilliQ H_2O (100 µl) and then quickly blown dry with Argon (inert gas). Multiple rinsing steps may be needed to eliminate salt in order to visualize the DNA Origami. Because distilled water denatures DNA, care must be taken to minimize their interaction time.

3.2 DNA ORIGAMI

3.2.1 Production and Annealing of CO_3970 DNA Origami

The CO_3970 DNA Origami was imaged using AFM to verify correct folding and

dimensions (Figure 14). Production of 10 nM CO_3970 DNA Origami, as diagramed

schematically in Figure 15, begins with a mixture of ssDNA oligonucleotides called staple

strands (50 nM)(purchased from IDT) and viral M13mp18 DNA (10 nM)(purchased from Bayou

Biolabs) which was brought to a volume of 50-100 µL using 1x TAE buffer solution containing

40 mM Tris base at a pH 8.0, 20 mM acetic acid, 1 mM EDTA and 12.5 mM $MgCl_2$. The

constructs were annealed using a BioRad Thermalcycler (T100), which enables the controlled

temperature decrease from 90 to 20°C over a 6-hour period. This is a variation of the original
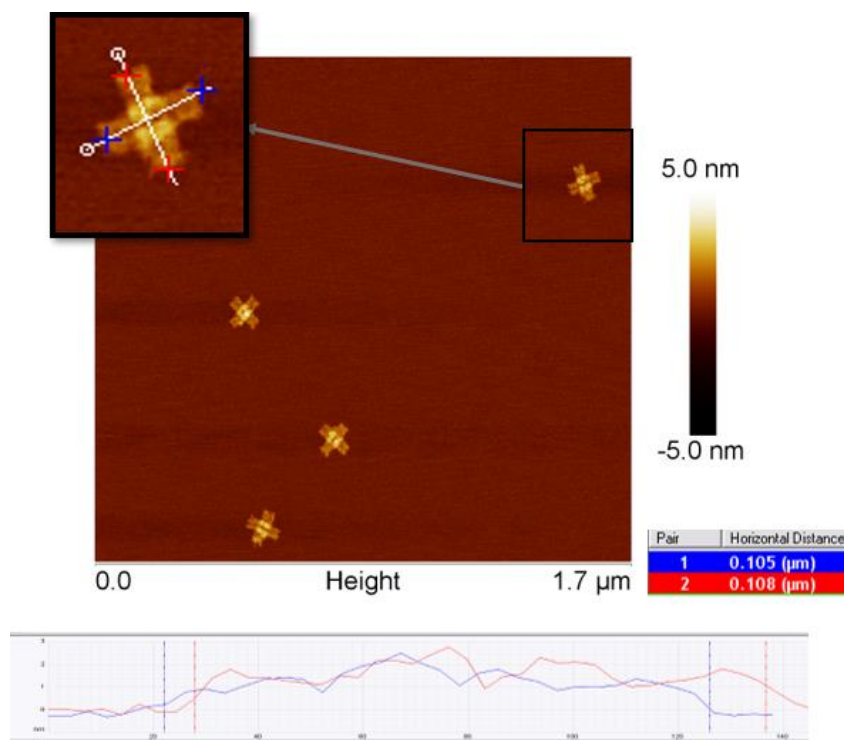
Figure 14 – AFM image and analysis of unmodified CO_3970. The single CO_3970 in the black outline was analyzed using Bruker Nanoscope Analysis and displays the approximate ~100 nm cross-section through the arms of a typical cross shaped origami. HPLC Purified.

annealing protocols.[8] Excess staples are removed from solution by centrifugal filtration

(Millipore 30 kDa filters).

The viral M13 DNA scaffold concentration is the limiting reagent of the DNA Origami

solution. When DNA Origami was first created, the researchers used ratios of staples to M13 up

to hundreds of copies of each staple in a set per M13 strand[5] to maximize the product. The

practice in the Norton lab is to use 5 staple sets per M13 strand. However, creating an LFA using

Temperature Ramp	Time Duration (sec)
90°C > 70°C	2min/degree
70°C > 45°C	10min/degree
45°C > 20°C	5min/degree
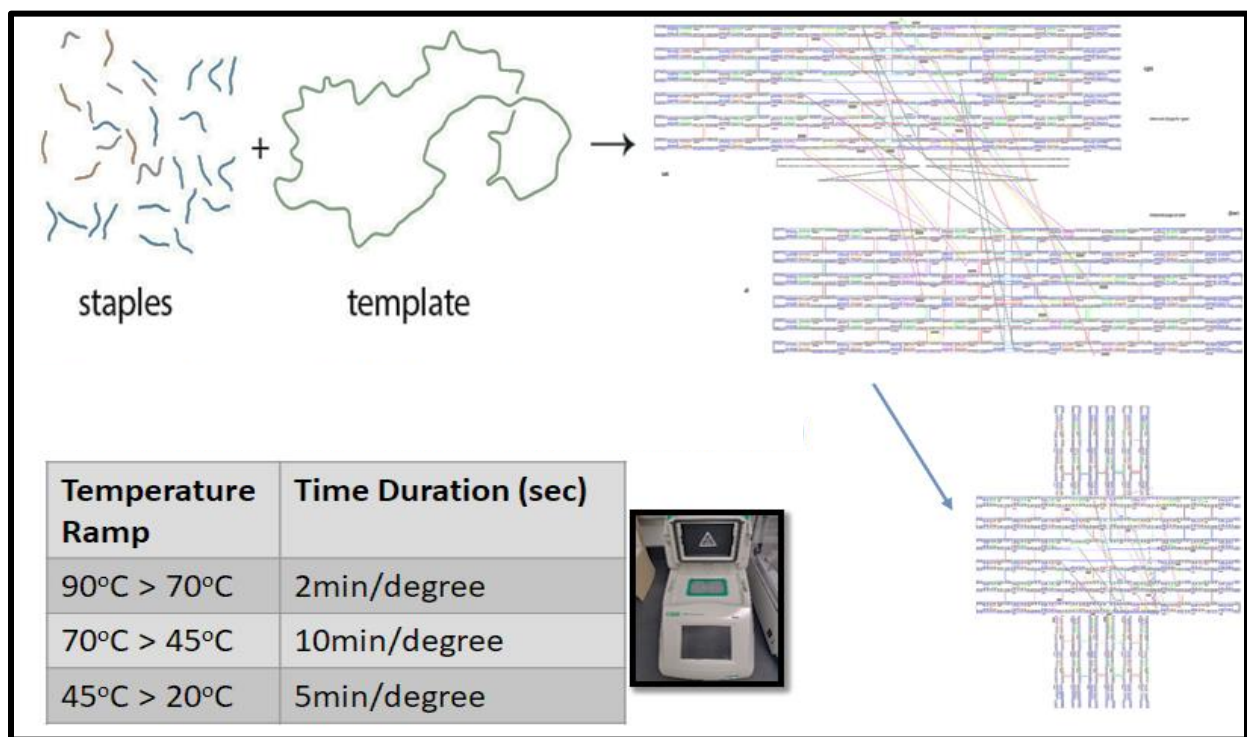
Figure 15 – Scheme of formation of DNA Origami. Displays the contents involved in the final Origami solution (i.e. the viral ssDNA-M13 template and shorter ssDNA staples in standard Origami buffer) which is heated to 90°C and slowly cooled to 20°C over the course of 6 hours. The staples have different crossovers to create specific shapes using ssDNA starting materials.

DNA Origami calls for amounts of material similar to those used in antibody LFAs which means

increasing the concentration of product. The standard of practice is to add 0.5-1 mg/ml (1-3 µl)

of probe to the analytical membrane.[40] To achieve these amounts, highly concentrated DNA

Origami solutions needed to be produced (100 nM-200 nM of the CO_3970).

21

In order to lower cost and apply the probe more efficiently, an experiment was conducted

to see if proper structure could be achieved using even fewer staple-sets per M13 strand. Origami

prepared with ratios of 1-5 staple sets per M13 were characterized using gel electrophoresis and

AFM imaging to confirm construct quality (Figure 16 and 17). Lane 5 in the gel corresponding

to a 3 staple-set per M13 DNA Origami solution provided the greatest signal. The 1:3
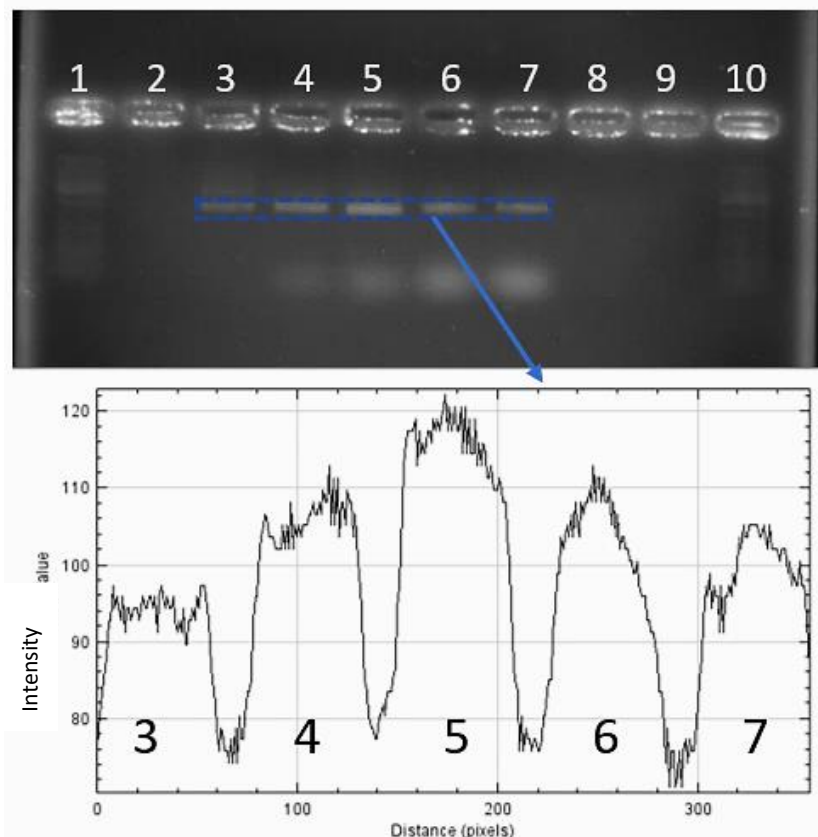
Figure 16 – Gel and intensity plot depicting M13 and staple set ratio optimization experiment.
CO_3970 band with lane 5 (1 M13 to 3 staple sets ratio) is the most intense. 1% Agarose (50 mL
1xCOB – 0.492 g Agarose). Lane 1 and 10: 2 µl Genelink Ruler + 2 µl Loading dye, Lane 3: 1:1,
Lane 4: 1:2, Lane 5: 1:3, Lane 6: 1:4 and Lane 7: 1:5. 2 µl of sample loaded + 2 µl of 80%
glycerol loaded in lanes 3-7. Same mass added per well - 2E-6 l x 2E-8 moles/l x 4.8E6 g/mole =
~186 ng per well.

(M13:staple-set) solution, which was used in the gel, was then imaged using AFM microscopy to

further confirm intact structure formation (Figure 17). Making concentrations upwards of 50-60

nM CO_3970, which is necessary to achieve the suggested concentrations required for

22

fabrication of an LFA, is more practical using this ratio. This analysis suggests that using the 1 to 3 ratio for all subsequent experiments is optimal.

3.2.2 Purification Methods of DNA Origami (exclusion of excess staple strands)

The CO_3970 DNA Origami solutions are filtered using 30 kDa MW centrifugal filters (30kD MWCO filters, Millipore, Bedford, MA). The Origami solution is added to filtration cartridges, which pass the smaller individual staples from the solution, with 2-3 additions of 400 µL of 1x DNA Origami buffer (1xTAE, 12.5 mM $MgCl_2$) after centrifugation for 5 min at 14800 RCF (12000 RPM). After 2-3 buffer additions, the filter is inverted in a clean tube and centrifuged for 2 min at 930 RCF (3000 RPM) which gives the purified contents. The solution
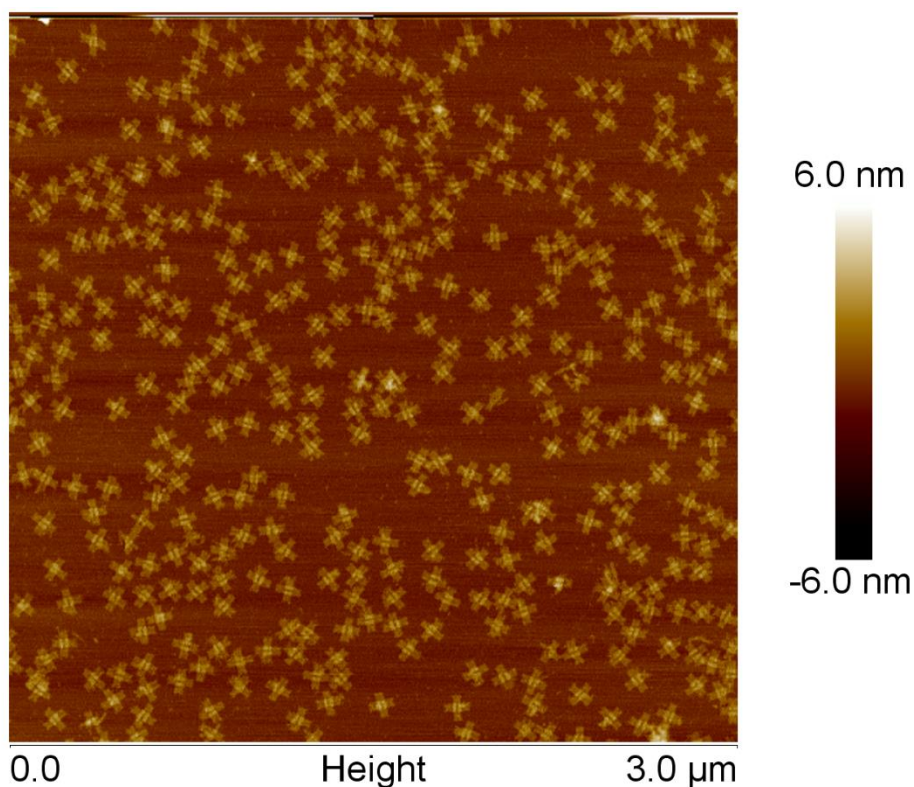
Figure 17 – AFM image of 1:3 ratio of M13 to staple sets. AFM image of CO_3970 structure created using a 1 to 3 ratio of M13 to sets of staples incorporated into the initial mixture. The ratio has been analyzed by gel electrophoresis and AFM to prove that DNA Origami can form under these conditions. The concentration of M13 for these tests was 20 nM and when concentrations are increased the kinetics of binding will increase as well. Of ~330 total cross Origami structures only 12 were notably not well-formed.

can then be analyzed for its concentration of DNA by using the DNA UV-Vis spectrometer

setting on the Nanodrop 1000 to obtain (ng/µl) concentration by analyzing the absorption peak at

260 nm. After filtration, the solution is stored at 4°C for preservation or used immediately.

A second, more complete way to purify DNA Origami is to run the sample through an

HPLC (high-performance liquid chromatography) apparatus.[41] The process, depending on the

type of column, will separate and purify all of the different structures in the sample. Using a size

exclusion HPLC column, structures of different molecular weight in the sample were collected

after different times spent in the column. The larger the structure the faster it eluted from the

column due to the small pore size of the column used. The CO_3970 was purified via HPLC and
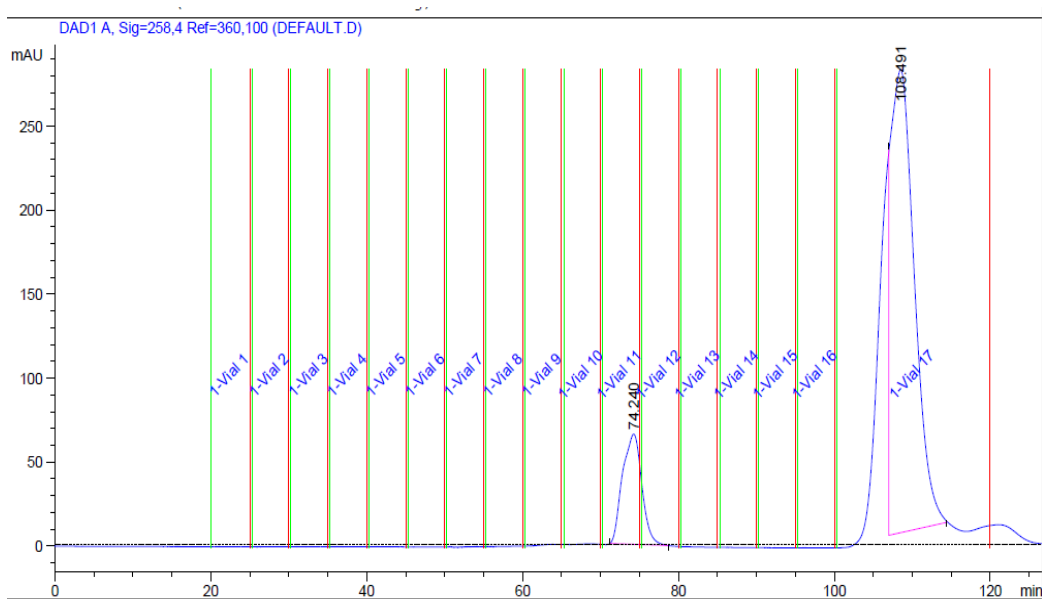
Figure 18 – HPLC spectrum of 20nM CO_3970 sample. Using a size exclusion column this spectrum was obtained. Fractioned from 20-120min with 5min per fraction. Parameters: Volume – 45 µl, Temp – 23°C, Flow rate – 100 mL/min and Buffer – 1xCOB. Pure CO_3970 obtained from fraction 11-12 peak (70-80 min). Column type is proprietary information.

the elution spectrum was obtained (Figure 18). However, a disadvantage to this purification

method is that the pure solution obtained is diluted to an extent which prohibits the necessary

concentrations for LFA creation.

3.3 MOBILE REPORTER AND IMMOBILE PROBE PREPARATION

3.3.1 Gold Nanoparticle Functionalization

Functionalization of the AuNPs begins with choosing the appropriate sequence for the thiolated oligonucleotide. The method and optimization of functionalization was tested using gel electrophoresis as shown schematically in Figure 19. The AuNPs were functionalized with this ssDNA sequence in order to bind to modified staple docking strands which extend from the DNA Origami surface. The thiolated ssDNA (ordered from IDT, Inc.) is rehydrated in MilliQ H_2O to produce stock solutions of the strand. In solution the thiol groups form disulfide bonds, which need to be reduced. A solution of Tris(-carboxyethyl)phosphine (TCEP), a suitable and
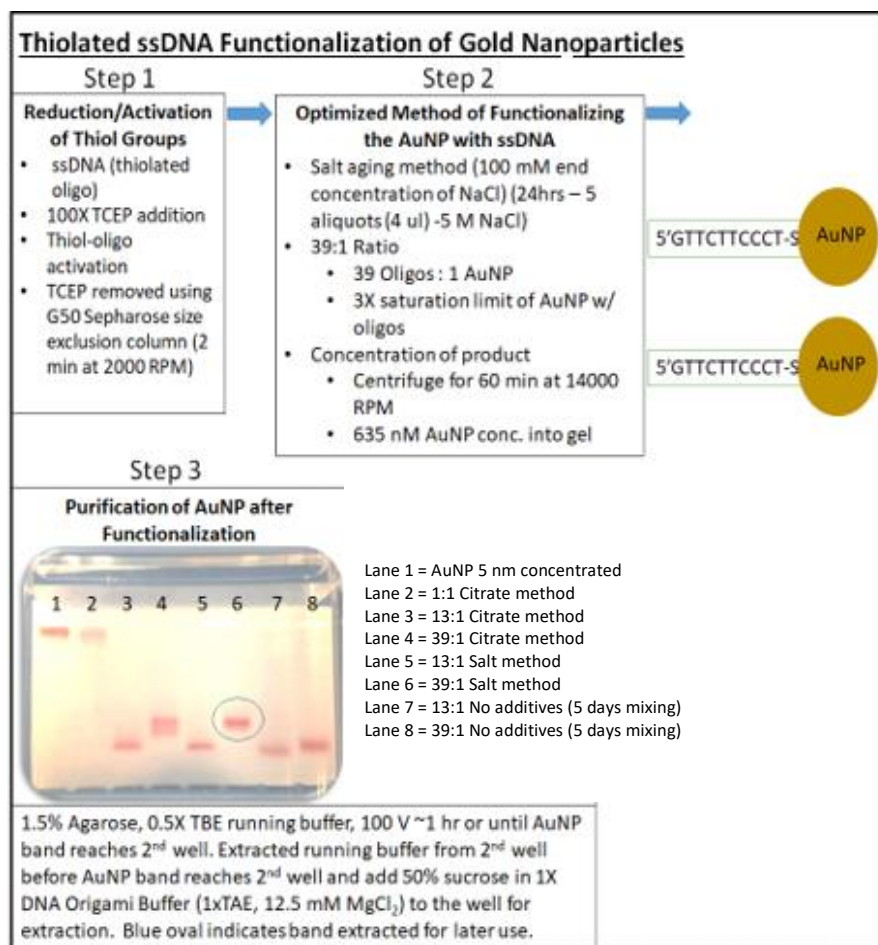
Figure 19 - Scheme of optimization of functionalizing AuNPs with thiolated ssDNA. Process begins with reduction which activates the sulfhydryl group. The activated thiol-oligos are then added to the AuNPs at saturating concentrations.[37] Using different methods of functionalization[33,38] the optimal method was determined by analyzing the product bands observed in agarose gel electrophoresis. Lane 6 shows the optimal method which was the salt-aging method at 39 oligos to 1 AuNP ratio. The oval drawn around the band indicates the band extracted for use.

widely used reducing agent, was added to the ssDNA at 100X of the concentration of DNA.[42] The TCEP was removed from the solution by G-50 Sepharose size exclusion centrifugation columns (GE Company). The reduced and purified thiol-oligonucleotides were then added to the 5 nm AuNP (Ted Pella-BBI) at specific ratios near or above the ssDNA loading capacity of 5 nm AuNPs.[36,42-44] The loading capacity has been reported to be at 13 ssDNA oligos per 5 nm AuNP (Table 1), ratios up to a 39:1 ratio (3X loading capacity) of thiol-oligonucleotides were added to the AuNPs.[37]

After addition of the ssDNA, different methods of functionalization (salt-aging, fast-citrate or no additives) were used for chemisorption of the activated, reduced thiol groups to the

d(Au) [nm]	number of bases per DNA	maximum number of DNA molecules per Au particle	maximum DNA density on the particle surface [nm^{-2}]
5	8	13	0.041

Table 1 - Thiolated ssDNA loading capacity on a 5nm AuNP. Table displaying data obtained from multiple gel electrophoresis studies of the loading capacity of 5 nm AuNPs from Alivasatos Lab.[37]

AuNPs.[37,38,45] The optimal method was found to be a salt-aging method.[31] Aliquots of 5 M NaCl were added to the mixture of ssDNA and AuNPs to give a final concentration of 100 mM NaCl after 24 hours of continuous mixing (Figure 19). After the functionalization step is complete, the AuNPs are concentrated by centrifugation for 80 minutes at 20000 RCF (14000 RPM) and purified using gel electrophoresis. A 1.5% Agarose gel with two rows of wells separated by 2 cm was used for purification, with 0.5X TBE running buffer, and run at 100 V for about 1 hour or until the AuNP band reaches the 2nd well. The electrophoresis was allowed to run until bands are close to the 2nd set of wells at which the running buffer is extracted from the well before the

AuNP band reaches that well. A solution of 50% (w/v) sucrose (standard preserving component for functionalized AuNP by the Norton lab) in 1X DNA Origami Buffer (1xTAE, 12.5 mM MgCl$_2$) was added to the well for extraction. Once the band reaches the well, the voltage across the system is paused for safety. 40-50 µl of the AuNPs are then removed from the well by pipette with at least a 50 µl capacity using 200 µl capacity tips (TipOne). Once purified via gel filtration, the AuNPs are ready for use in DNA Origami solutions.

This method was adapted for the necessary concentration needed to facilitate creation of the LFA. The only alteration in the protocol for this adaptation is the centrifugation of AuNPs before functionalization. The nanoparticles are centrifugally concentrated twice before running through agarose gel for purification in order to achieve the highest concentration possible in the final product.

3.3.2 Preparation of DNA Origami with Functionalized AuNPs

After AuNP functionalization, these AuNPs were added to a solution containing the purified, modified CO_3970 Origami construct (Figure 12) to give a 3 to 1 ratio of AuNPs to DNA Origami. Also, the solution had a final concentration of 100 mM NaCl to help drive the hybridization reaction and reduce charge repulsion. The solution was annealed in a BioRad Thermalcycler for ~2 hrs from 45-20℃ (decreasing in temp by 1 degree/5 minutes). Drop dialysis was performed against 1xCOB using a Millipore nitrocellulose dialysis membrane (pore size: 0.025 µM) to exchange the high NaCl concentration as DNA Origami does not bond strongly to mica at high NaCl concentrations due to charge shielding. Once the NaCl was exchanged from the solution, an appropriate amount (10 µl of ~1 nM DNA Origami) is deposited onto mica and then imaged using AFM. Once this assembly verification procedure is complete,

this construct, named the mobile reporting probe, can be mixed with a preserving mixture and deposited onto the conjugate pad.

3.3.3 Preparation of Tris-NTA: Fluorescent Protein Complex (AFM Imaging)

The Tris-NTA modified CO_3970 Origami construct was complexed with His-tagged mCherry fluorescent protein by first adding $NiCl_2$. The $NiCl_2$ was added to the modified 1nM CO_3970 Origami at a 10X concentration to give 1 DNA Origami to 10 $NiCl_2$. The mixture was allowed to react at RT for 30 minutes. The mCherry fluorescent protein was then added to this mixture at a 5X concentration to the Origami. The mixture was then allowed to react at RT for 48 hours. An appropriate amount (10 µl of ~1 nM DNA Origami) was deposited onto the mica and then imaged using AFM. These experiments were performed to evaluate the ability of the fluorescent protein to complex with the transition metal bound to the Tris-NTA available on the surface of the DNA Origami (Figure 8).

3.3.4 Streptavidin-Biotin Interaction

Biotinylated staple strands on the right arm of the capture probe serve as the mechanism to immobilize the capture probe onto the analytical membrane. The interaction of Streptavidin and Biotin has been widely studied and is found to be an efficient way to immobilize structures onto Nitrocellulose membranes due to an inherent affinity for proteins.[46,47] Mutant streptavidin synthesized specifically to bind better to nitrocellulose (more hydrophobic interaction) was purchased for our experiments (ProSpec). The Streptavidin is mixed at a ratio of 10-30 proteins (depending on the construct design) per 1 CO_3970 and kept at 4°C for 2 hr.[47] The preincubation of Streptavidin and the biotinylated capture probe was previously found to be the most effective way to immobilize a species onto NC using this protein adsorption technique.[16] This procedure

28

allows enough time for the reaction to take place between the two species. Once Streptavidin is bound to the capture probe, the solution can be deposited onto the analytical membrane.

3.4 TEST STRIP PREPARATION

3.4.1 Nitrocellulose Selection and Preparation

Membrane selection was based on the properties, such as pore size, of the membrane. The name of the membranes usually provides information about capillary flow which in this case designates how many seconds it takes liquid to laterally flow through 4 cm of the membrane. The larger the pore size the faster the liquid flows through the membrane (Table 2). The incubation time between the capture probe on the membrane and the reporting probe flowing through the membrane is decreased the faster the flow rate is. Given that some information, including pore sizes, is proprietary from each vendor, the medium flow rate membranes were chosen for the ensuing experiments due to the large size of the cross-shaped DNA Origami and ability to enable the longest possible incubation time between species which should increase sensitivity.

Relative Flow Time (capillary flow rates s/4cm)	Relative Pore Size	Relative Sensitivity	Examples (in hand)
Fast	Large	Low	Millipore: HF 75, 90 Sartarius: CN 95 Whatman: FF80HP
Medium	Medium	Medium	Millipore: HF 120, 135 Whatman: FF120HP
Slow	Small	High	Millipore: HF180

Table 2 – Properties of nitrocellulose (NC) membranes. A table describing the properties of the nitrocellulose membranes which are available in kit (DCN Diagnostics, Inc.).

An experiment was conducted to ensure strong binding between the streptavidin and the

nitrocellulose as this is the technique being utilized to immobilize the capture probe (Figure 20).

The experiment involved immobilizing 4 µl of 1 µg/µl Streptavidin onto various membranes to

test the adsorption capabilities of the membranes by dyeing the protein with Ponceau and then

rinsing the dye off to reveal protein staining. Of these selected membranes, the medium pore size
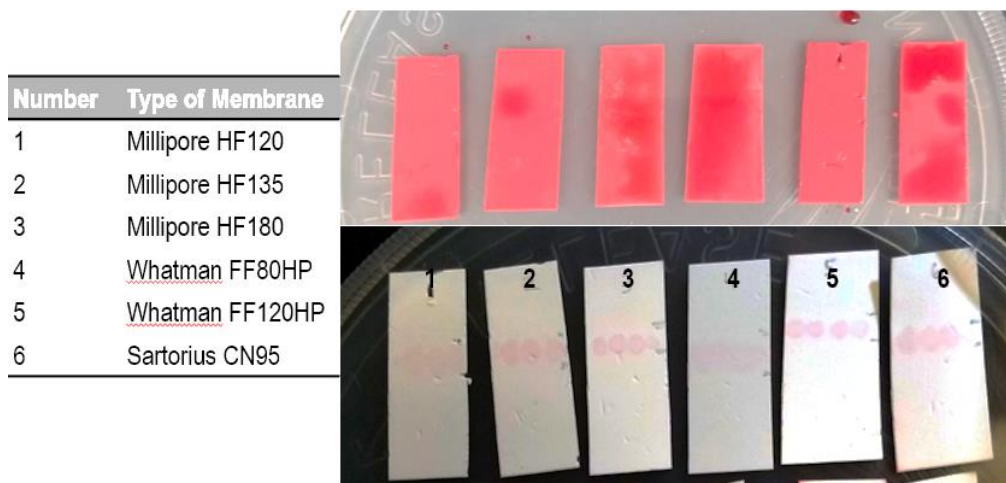
Figure 20 – Testing NC membranes for protein immobilization (Ponceau dye stained SA). Ponceau dye stained Nitrocellulose with Streptavidin immobilized onto the membrane. Dye was rinsed and protein still immobilized was visible as spotted pink lines.

membranes were chosen, and the most intense protein band and least diffuse line was observed

in the Whatman FF120HP membrane. The Whatman FF120HP membrane was then used in

subsequent tests described here.

3.4.2 Control Line Preparation and Application

After membrane selection, the next step in the process was to prepare and deposit the

control line onto the analytical membrane. The capture probe, deposited at the control line,

consists of DNA Origami modified to enable the three separate versions of possible LFAs: 1)

CO_3970 with 6 polyT(10) staples on the end of the left arm (Figure 21), 2) CO_3970 with

staple 15 modified with a Tris-NTA on the 5' end (Figure 8) and 3) CO_3970 with three

thrombin binding aptamers (TBA29) on the end of the left arm (Figure 22) all of which have biotinylated staples on the ends of the right arm to immobilize the probes onto the membrane. The version of the construct most studied in this thesis consists of the six polyT(10) staples and all optimization experiments were conducted using the ssDNA hybridization capture for testing of various non-analyte specific parameters and variables.
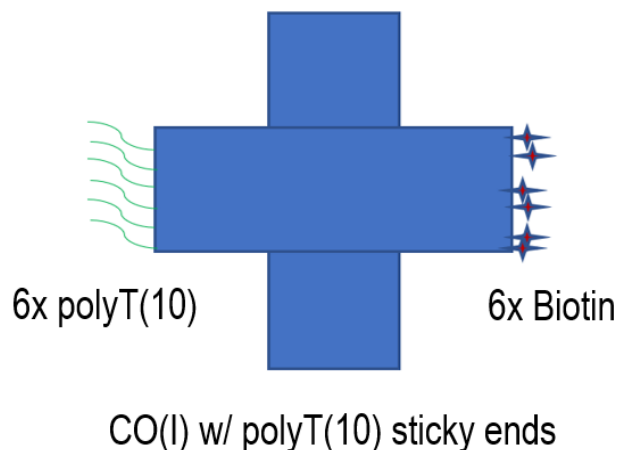
Figure 21 – Design of CO(I) immobile probe for ssDNA hybridization LFA. Using biotinylated staples on the right arm to immobilize the CO(I) after preincubation with Streptavidin. CO(I) construct is used for subsequent experimentation with DNA hybridization being the focus of the capture mechanism.
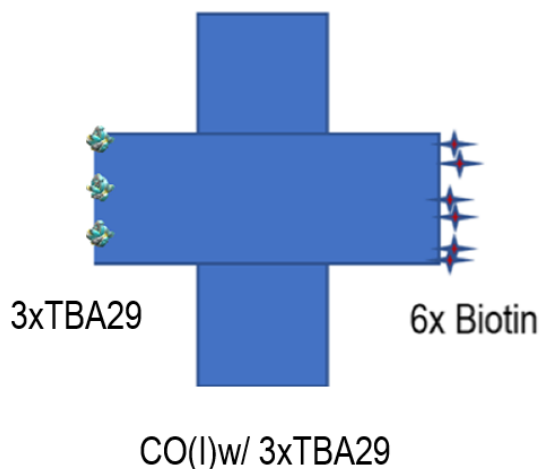
Figure 22 – Design of CO_TBA(I) immobile probe for the thrombin LFA. Using biotinylated staples on the right arm to immobilize the CO_TBA(I) after preincubation with Streptavidin. CO(I-TBA) construct uses TBA29 aptamer binding to facilitate capture of Thrombin protein. Aptamer sequences are provided in the supplementary information section.

The recommended control line probe concentrations when using an antibody is between

0.5-1.5 mg/ml, using 1-2 µl per test strip, so preparing the control line using DNA Origami

involves mixing and annealing a 50 nM solution of the immobile probe.[40] 50 nM corresponds to

a ~0.25 mg/ml solution. This probe containing solution is purified by Millipore centrifugal

filtration units (30 kDa) and then concentrated in an Eppendorf concentrator which evaporates

the water thereby concentrating the aqueous solution, so that the final concentration will be at or

near the recommended 0.5 mg/ml (~100 nM) when mixed with streptavidin. Prior to application

on the LFA, the concentrations of DNA Origami are usually between 100-200 nM and the

solution is then mixed with streptavidin to give a final concentration of 10x or 10 streptavidin to

1 DNA Origami.

Deposition of this capture probe and streptavidin solution can be accomplished in a few

ways. Initially, a system was set up to use a syringe pump apparatus for the deposition of the

control line (Figure 23). The method was explored and verified to be an acceptable deposition

method; however, due to the small-batch preparations used in prototype experimenting, the

syringe pump method will only be used when the optimal LFA design is defined. The rate of
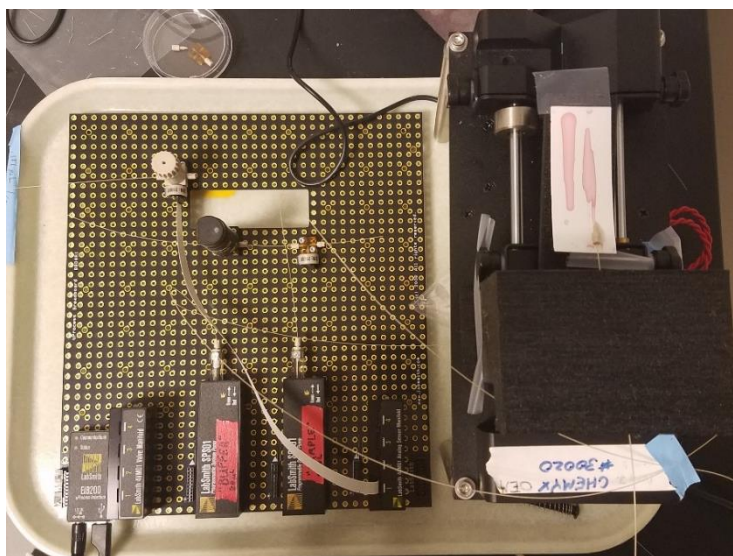
Figure 23 – Syringe pump apparatus with accompanying hydraulic mechanism.

flow of this apparatus allowed for deposition of 2 µl of solution per cm of membrane. To achieve

~1 mm line width, the syringe pump was calibrated with a translation stage mechanism to allow

for fast lateral movement across the membrane line deposition area at ~3.7 mm/s.

The alternative, used to deposit small batch solutions for experimentation, was to pipette

the capture probe solution directly onto the membrane. Experiments were carried out to find the

optimal way to deposit the solution and immobilize the probe onto the membrane. The initial
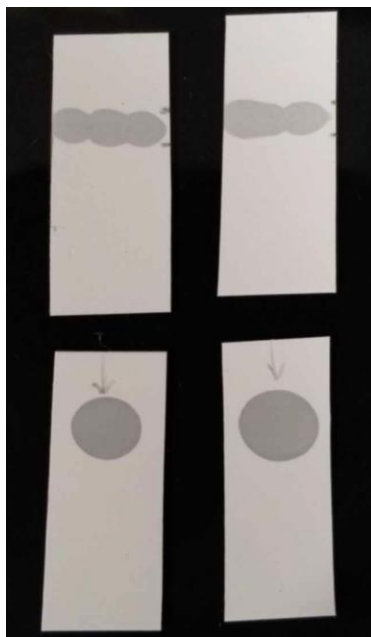
Figure 24 – Image of NC membranes in line or spot deposition experiment. Image of still damp
line (above) and spot (below) of deposited immobile capture probe. The solution was deposited
onto Whatman HF120. Membranes cut to 0.5x2.5 cm in this test.

experiment consisted of pipetting capture probe solution, with probe amounting to a mass in an

amount of weight comparable to an analogous LFA using antibody as the probe, onto the

membrane in the form of either a line or a spot pattern (Figure 24). The pipetted line was the

most suitable for ensuing testing because less reporting probe is lost to the flow around the spot

which makes the assay less sensitive.

Once a signal was achieved using the lateral flow of the mobile reporting probe

hybridizing with the ssDNA on the immobilized capture probe, the deposition method was

optimized by increasing the amount of probe deposited for increased signal intensity. Before

optimization of intensity took place the DNA Origami LFA was tested by using two capture

probe negative controls, one with no ssDNA hybridization strands and one with streptavidin

deposited alone (Table 3)(Figure 25).

In order to increase the signal, more immobile capture probe needed to be initially

immobilized onto the NC membrane. This increase in density was achieved by adding 2 µl of the

LFA	Immobile	Expected result	Observed result
1	CO(I) with 6 polyT sticky ends	+	+
2	CO(I) no sticky ends	-	-
3	Streptavidin	-	-

Table 3 – Control experiment parameters for ssDNA hybridization LFA. Table depicting the control experiment parameters in Figure 25.
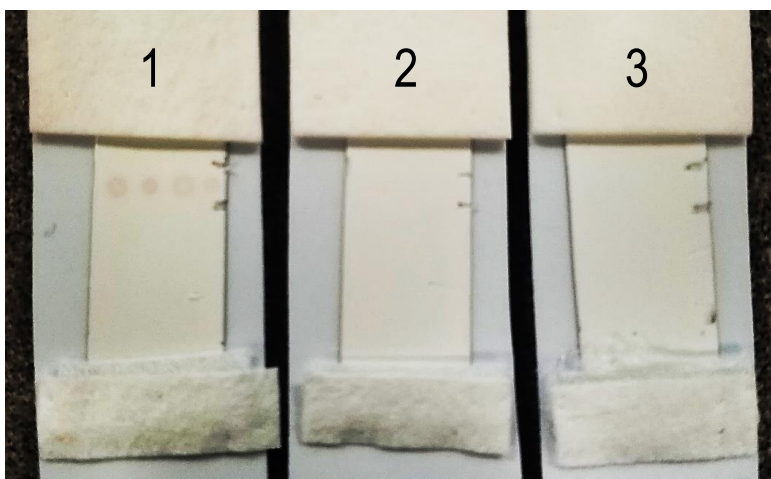
Figure 25 – Image of experimental control LFAs of immobile capture probe. Experimental control of immobile capture probe capabilities. The result is a positive test corresponding to the capture probe with hybridization strands. The other two controls were negative for capture of the reporting probe. Pencil marks on the right side of each membrane bracket the locations where immobile probe or protein was deposited across the membrane. Assay #1: positive control, #2-3: negative controls.

capture probe solution of 100-200 nM to a 0.5 cm wide NC membrane and allowing the solution

to dry for 10 minutes at ambient room temperature (~21°C), then depositing another 2 µl of the

same solution in the exact same area and repeating this until a total of 6 µl of solution is drying

on the NC membrane. This approach minimizes the width of the deposited line while tripling

mass deposited of immobile capture probe.

After an increase in deposited capture probe was implemented successfully, the next

parameter of the immobilization technique to be considered was how to dry the membranes for

optimal adhesion of the streptavidin-labeled probe onto the NC membrane. To test different

techniques, 5 µl of 15 µM streptavidin solution stained with Ponceau dye was deposited in a line

onto three NC membranes (Figure 26). The membranes were dried using a drying protocol of

either 1 hr, 2 hrs at 37°C which were followed by either storage under desiccation overnight, or

~20hrs at 37°C before use.[47]
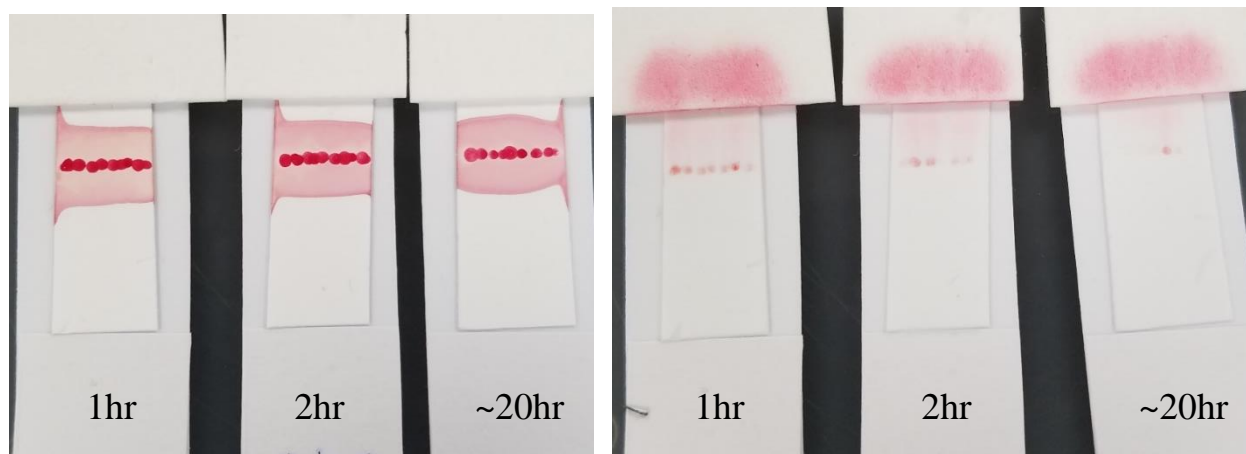
Figure 26 – Testing immobilization techniques on NC (Ponceau dye stained SA). 5 µl of 15 µM Ponceau dyed mutant nitrocellulose-binding Streptavidin was deposited onto a membrane and immobilized in three ways: 1) 1 hr at 37°C and overnight in a desiccator, 2) 2 hrs at 37°C and overnight in desiccator and 3) ~20 hrs in 37°C. After immobilization techniques, 1xCOB was laterally flowed through the system. Before (left) and after (right) images.

Experiments conducted to optimize the control line deposition and immobilization

techniques have led to a consistent method used in future tests shown here, all consisting of these

optimal protocols: 1) the capture probe solution must be at or near 100 nM (0.5 µg/µl) and preincubated with Streptavidin for at least 2 hrs at 4°C before deposition, 2) the best deposition technique is to deposit the capture probe solution 2 µl at a time, allowing 10 minutes of drying between each, to give a total deposition of 6 µl in a line and 3) for best immobilization of the capture probe, the NC membrane must be heated for 1 hr at 37°C and placed in a desiccator overnight. Once deposition and immobilization are complete, the next step of the process is to block the conjugate pad to optimize release of the mobile reporting probe and block the analytical membrane to prevent adhesion of the mobile probe to the membrane allowing subsequent capture of the probe at the control line.

3.4.3 Blocking the Analytical (NC) Membrane

Blocking the membrane against unwanted interactions is a pivotal step to achieve the highest specific signal by avoiding non-specific binding of the mobile reporting probe. If the probe indiscriminately binds to the NC membrane while traveling through during the lateral flow step, the test as a whole will be less sensitive. Many blocking techniques have been studied previously.[14,48] The method developed here blocks the membrane using PBS buffer with 1% BSA (w/v) and 0.2% Tween20 (w/v).

3.4.4 Conjugate Pad Preparation

The mobile reporting probe consists of two types of modified DNA Origami or a fluorescent protein to give the three separate capturable probes for different versions of LFAs: 1) CO_3970 with six polyA(10) staples on the end of the right arm (Figure 27), 2) a His-tagged fluorescent protein (Figure 8) and 3) CO_3970 with three thrombin binding aptamers (TBA15) on the end of the right arm; each of the DNA Origami constructs have three optically active

36
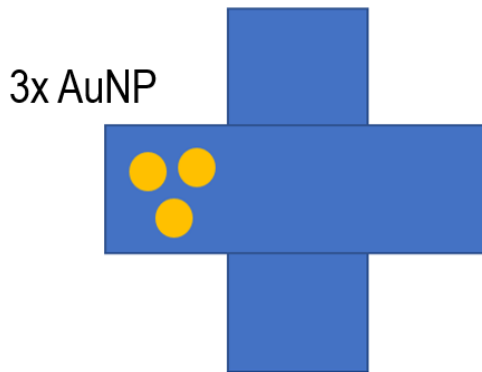
Figure 27 – Design of CO(M) mobile probe for ssDNA hybridization LFA. Mobile reporting probe designed with polyA staples on the right arm for capture at the CO(I) control line after release from the conjugate pad and lateral flow through the analytical NC membrane. CO(M) uses DNA hybridization as the capture mechanism. The only changes when using the CO(M)_TBA LFA is to substitute three TBA15 strands for the polyA strands.

AuNPs on the left arm in order to display a signal when captured at the control line (Figure 27). The version most studied in this project consists of the six polyA(10) staples and all experiments optimizing the LFA for flow and concentration characteristics were conducted using the ssDNA hybridization capture for testing of various parameters and variables.

3.4.5 Preservative Solution and Deposition

Many different preservative solutions containing sucrose, BSA and Tween20 have been proposed for many different varieties of conjugation reporting probes.[14,16,49,50] The preservative components are mixed with the probe solution at various concentrations. Optimization of this mixture allows the probe to easily dissociate from the conjugate pad upon rewetting and also stay intact and viable for extended periods of storage time. The preservation solution composition identified here which worked effectively, (when mixed with reporter probe solution) is 20% sucrose, 1% BSA and 0.25% Tween20. These preservative components of typical LFAs were individually tested by combining them with DNA Origami in solution to determine whether there

were any negative effects observed. The solutions were imaged using AFM after 24hrs of

incubation at room temperature. Sucrose and BSA have previously been tested with DNA

Origami in the Norton lab and were found to not have any negative effects. However, Tween20

had not been tested for interactions with DNA Origami. Hydrophilic surfactants, such as
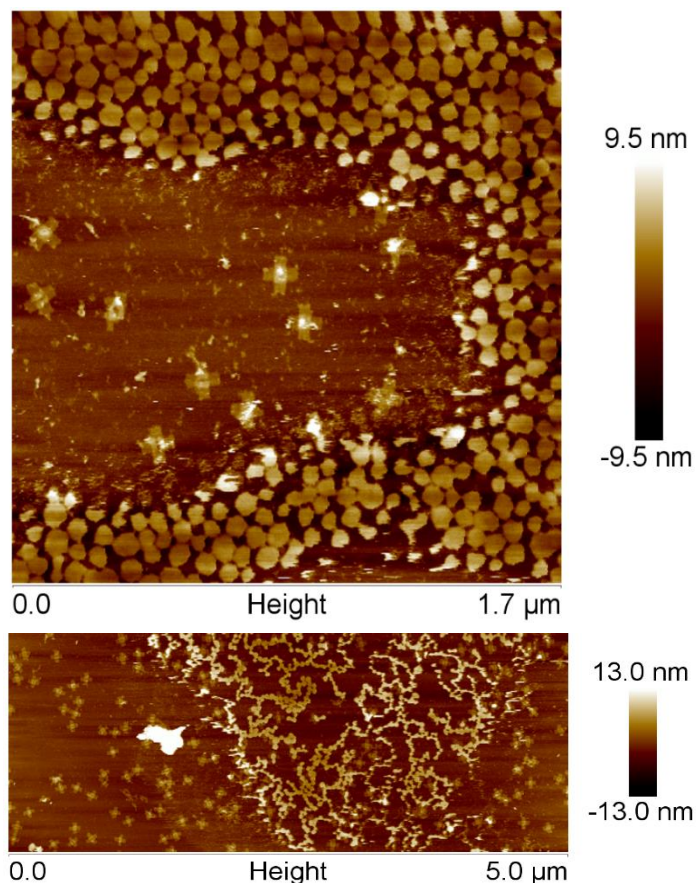
Figure 28 – AFM images of DNA Origami in solution with Tween20. Two images of different areas of the Tween20 sample deposited onto mica. All well-formed DNA Origami showed typical 100nm length and width. The Tween20 seemed to have no negative effect on CO_3970 DNA Origami. In the top image, micelles of Tween20 were observed in the periphery of the image, around the Origami.

Tween20, help biomolecules to maintain their proper function and can reduce the nonspecific

interactions between DNA-modified AuNPs and solid materials.[50] An extreme concentration (8%

w/v) of Tween20 was added to a 2 nM solution of DNA Origami for 24 hrs then imaged (Figure

28). Tween20 had no visible negative effects on DNA Origami thus it has been used in all complete LFA devices and can be used in the conjugate pad preservative mixture.

Experiments were also conducted by applying DNA Origami in preservative solutions onto NC membranes and drying them for certain defined times to demonstrate their preserving abilities. NC membranes, after drying for 3 days at 37°C, were then rehydrated in 1xCOB

Lane Sample	1 ssM13	2 BSA 2% on NC	3 BSA 2% in solution	4 Tween20 8% on NC	5 Tween20 8% in solution	6 Sucrose 20% on NC	7 Sucrose 20% in solution	8 P4 on NC	9 P4 in solution	10 CO_3970
Concentration	10nM	2nM*	2nM	2nM*	2nM	2nM*	2nM	2nM*	2nM	2nM
Volume (not including glycine)	6uL	10uL	10uL	10uL	10uL	10uL	10uL	10uL	10uL	10uL
Mass loaded	144ng	230ng	230ng	230ng	230ng	230ng	230ng	230ng	230ng	230ng

Table 4 – Preservative component mixtures for gel electrophoresis experiment. Preservative components mixed with CO_3970 and either dried at 37°C on nitrocellulose for 3 days and rehydrated, or maintained in solution for 3 days. Lane 1 and 10 are controls. P4 in lanes 8 and 9 corresponds to the solution composition (20% Sucrose, 1% BSA, 0.25% Tween20) for which AFM images reflected recovery of intact sample after drying on NC. Table shows mass of each sample loaded into the gel. *Expected Molarity after rehydration in solution for 2 hours.
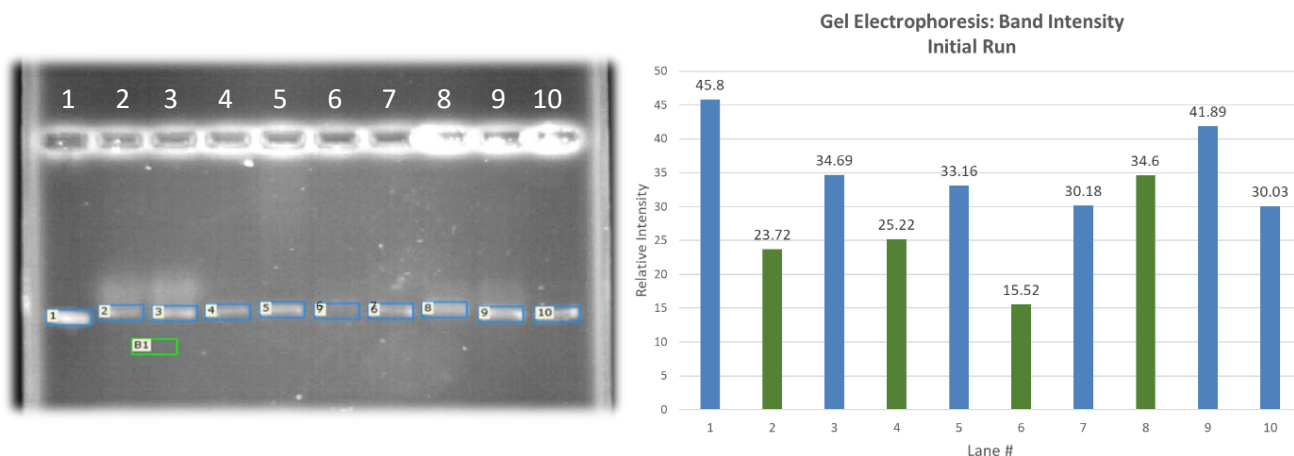
Figure 29 – Gel analysis of preservative component mixture optimization experiment. Image of 1% agarose gel (left) and analysis chart (right) showing that the preservative components mixture P4 yields the highest recovery of materials from the NC membrane after rehydration (Lane 8). Together these components enhance the ability to disperse DNA Origami constructs back into solution after they are dried onto a membrane for storage. Blue columns = in solution. Green columns = rehydrated from NC membrane. Green rectangular section in gel, denoted as B1, is the background value which was subtracted from each band intensity value.

solution (2 hours) or in 1xCOB buffer solution for 3 days. Gel electrophoresis was used to decipher the effects of these on the structure and recovery yield of the DNA Origami (Table 4, Figure 29).

After the preservative mixture for the conjugate pad was demonstrated to successfully allow the dissolution of probe back into solution, the preservative mixture and the reporting probe of the conjugate pad were ready to be mixed together. AFM images of the 6 polyA hybridization CO were obtained to ensure proper binding and good yield of binding of AuNPs (Figure 30). Once the proper binding was confirmed for the AuNP sites, the Origami probe was then produced at the higher concentrations required for LFA studies. The method for the mobile reporting probe preparation begins with mixing a 50 nM solution of the correct DNA Origami
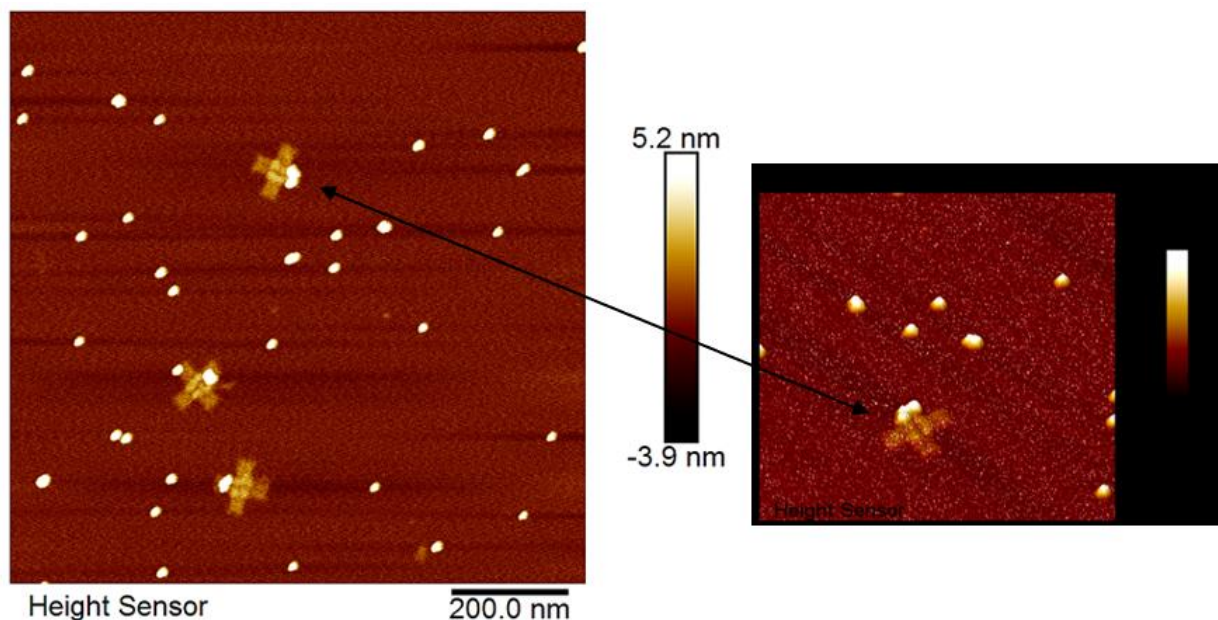
Figure 30 – AFM images of CO(M) mobile reporting probe for ssDNA hybridization LFA. The AFM images display proper binding of the 3 AuNPs. This sample was a mixture of 1 CO_3970 to 10 AuNPs (2 nM CO : 20 nM AuNP) and 100 mM NaCl and annealed from 45 to 20°C over 2 hours.
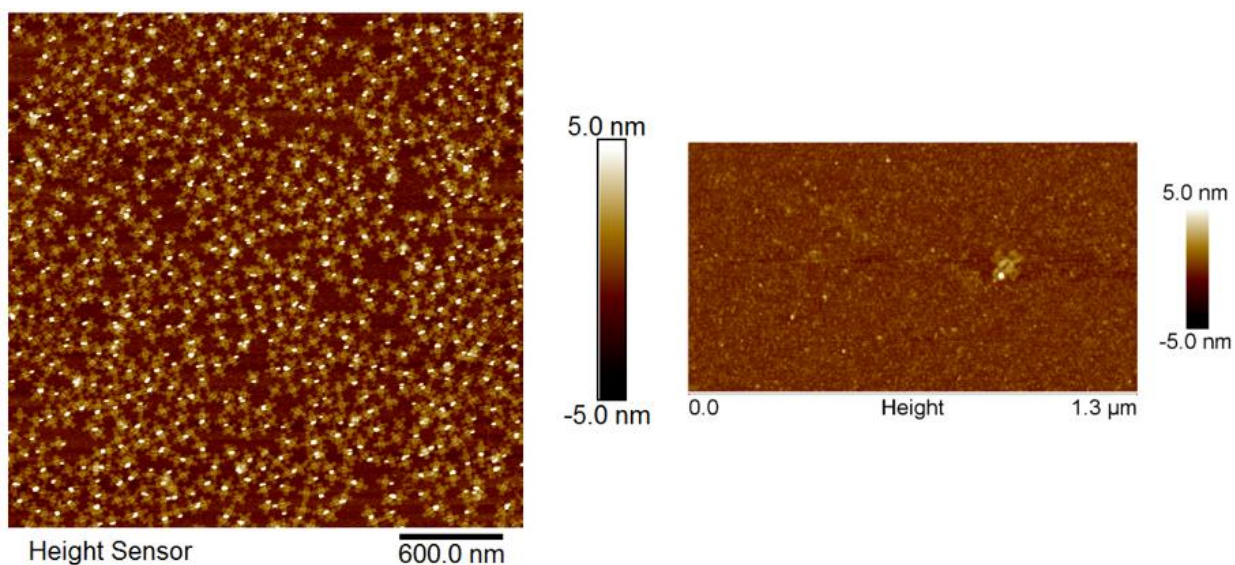
Figure 31 – AFM images of concentrated CO(M) and reconstituted CO(M). Left image: AFM images of mobile reporting probe after concentration in Eppendorph concentrator. 99% of CO_3970 decorated with at least one AuNP. Right image: reconstituted CO(M) in preservative mixture which had been dried on conjugate pad.

version of the probe, centrifuge filtering the excess staples from the solution, mixing with AuNPs at a 1:3 ratio in 100 mM NaCl when working with higher concentrations, and annealing the solution from 45-20°C over a period of 2 hours. This solution is then concentrated using an Eppendorf evaporator (07-748-13) to remove water from the sample solution to concentrate the CO(M) probe to detectable levels necessary in an LFA setup. AFM images of the concentrated sample of CO_3970 decorated with AuNPs were obtained (Figure 31). The end result of mobile probe preparation allows for mixing with the preservative mixture and still having a viable concentration to dry in the conjugate pad.

3.4.6 Lateral Flow Assay Assembly

The protocol used for assembly of a complete LFA is presented below.

Analytical Membrane Preparation:
NC analytical membrane (Whatman FF120HP)
- 4 mm x 2.5 cm (cut using Swissors precision cutting scissors)
- 6 µl of concentrated immobile probe (100 nM-200 nM) pre-incubated with streptavidin (1:30 ratio for 1 hr at 4°C) deposited as a line onto the NC membrane
- Dried for 1 hr at 37°C then overnight in desiccator
- Positioned on backing card leaving room on bottom and top for conjugate and absorbance pad respectively

Conjugate Pad Preparation:
Conjugate pad (Ahlstrom 6615)
- 4 mm x ~1 cm (cut using Swissors precision cutting scissors)
- 20-30 µl of mobile probe with preservative solution (40 nM-100 nM) pipetted and allowed to saturate through the conjugate pad
- Dried for 1 hr at 37°C
- Assembled overlapping the prepared NC membrane on the backing card (overlapping the NC membrane ~3 mm)

Absorbance Pad Preparation:
Absorbance pad (C083 Millipore)
- 2.5 cm x 4 mm (cut using Swissors precision cutting scissors)
- Assembled by overlapping NC membrane on opposite side from conjugate pad (3 mm overlap)

Sample Pad Preparation:
Sample pad (Ahlstrom 1660)
- ~1 cm x 4 mm (cut to similar size as the conjugate pad) (cut using Swissors precision cutting scissors)
- Placed nearly overlapping the conjugate pad

4.1 ANALYSIS OF DNA HYBRIDIZATION LFA

AFM images were obtained before the lateral flow assays were run to confirm structure and function of both mobile and immobile probes. The probes were decorated with either AuNPs for the mobile probe or streptavidin for the immobile probe. The two different decorations made the probes easily distinguishable when analyzing with AFM imaging systems because streptavidin's diameter is 3.5 nm and the AuNP diameter is ~5 nm (Figure 32). The architecture and spacing of the two separate (mobile and immobile) modifications allow for different height and placement in the x and y axis of the two variations (Figure 33). The AFM analysis displays the ability of the two separate probes to hybridize in a short amount of time (2 minutes in solution). The AFM analysis was performed using minimal concentrations in order to test the functionality at low concentrations.
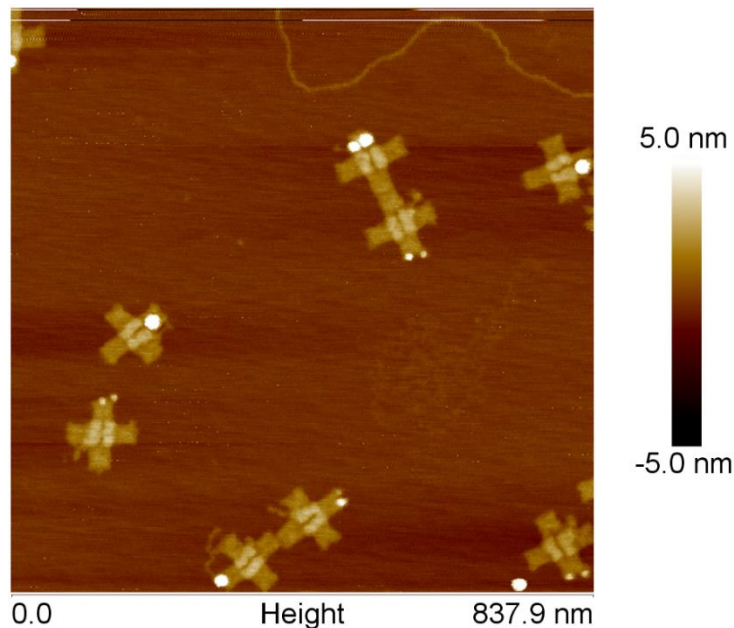
Figure 32 – AFM image of hybridized CO(M) and CO(I). Mobile reporting probe conjugated with the immobile capture probe. Mixed at 2 nM concentrations for 2 minutes then imaged.
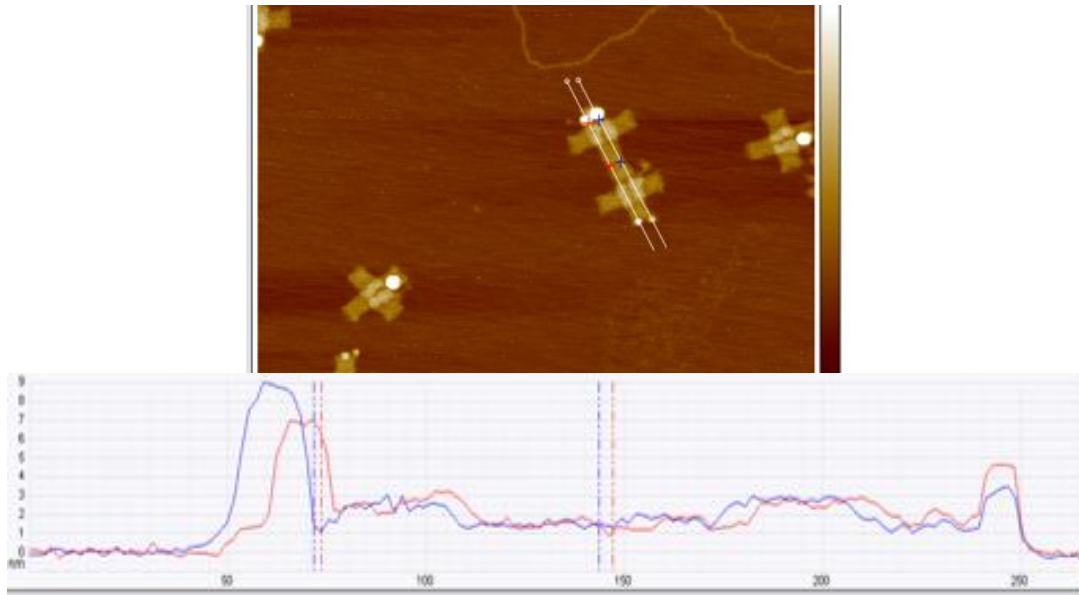
Figure 33 – Analysis of AFM image of hybridized CO(M) and CO(I). AFM images of mobile reporting probe conjugated with the immobile capture probe. Lower plot displays analysis of height and width of the two probes. 5 nm AuNPs are typically measured to be 6-9 nm in height when bound to CO_3970 and streptavidin typically appears to be 3-5 nm in height when bound.

	Ratio	Time annealing
CO(M)	1:5 (CO:AuNP)	2hrs:45-20C
CO(I)	1:5 (CO:SA)	0 min (mixed with final solution
CO(M)(I)	1:1	20min in solution
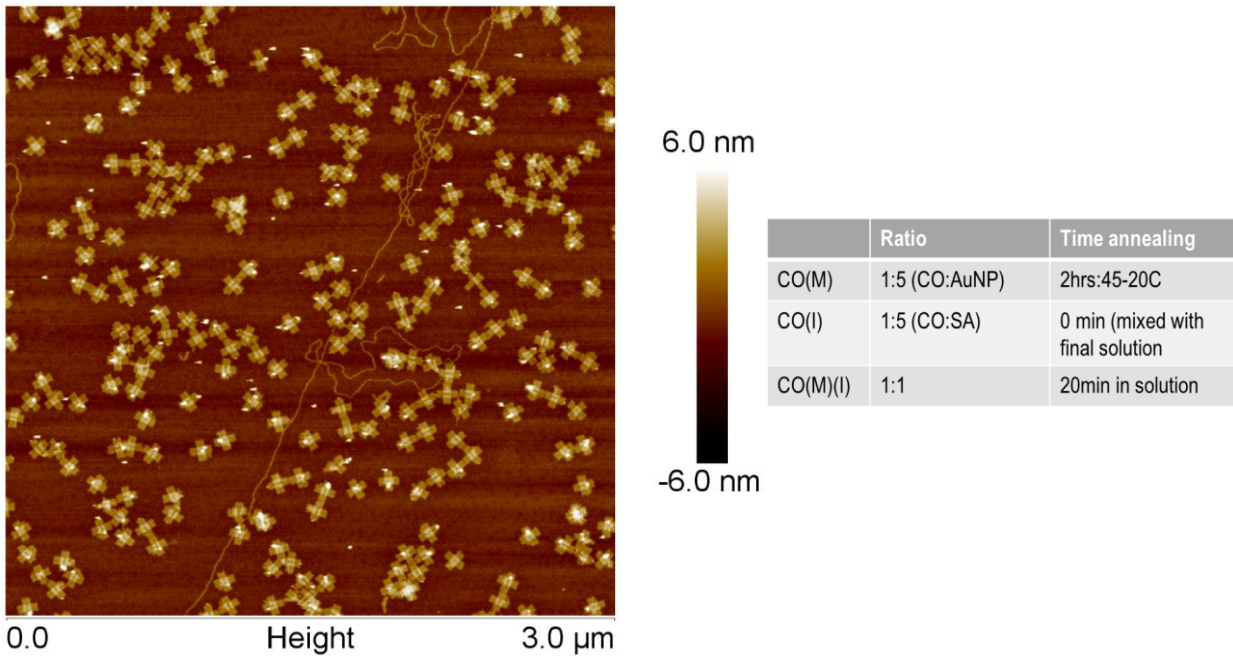
Figure 34 – AFM image of CO(M) conjugated to CO(I). Table showing variables and preparation techniques of the two separate probes. Confirmed 47 of 88 CO(M) with AuNP's bound to its CO(I) counterpart via ssDNA hybridization. 64 of ~200 total constructs confirmed unbound.
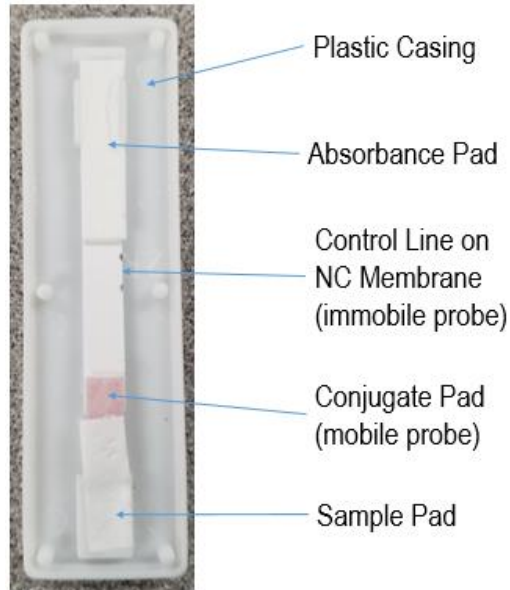
Figure 35 – Image displaying LFA component setup. Some experiments were performed using no plastic casing.

Confirmation of binding of the two constructs prompted the construction of the DNA hybridization based LFA. In the first tests performed using the whole system (all of the components of an LFA (Figure 35)) the immobile capture probe was deposited onto the NC membrane as either a spot or a line. The test was designed to compare two different immobilization thermal protocols, each using either a spot or line format deposited onto the
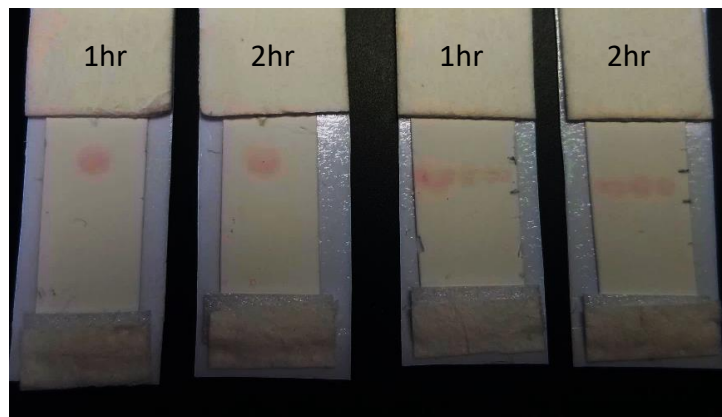
Figure 36 – ssDNA hybridization LFA – line or spot. ssDNA hybridization LFA testing different immobilization techniques in two different formats on the NC membrane. Solution of CO(I) was either dispensed in a spot (left pair) or a line (right pair) across the membrane.
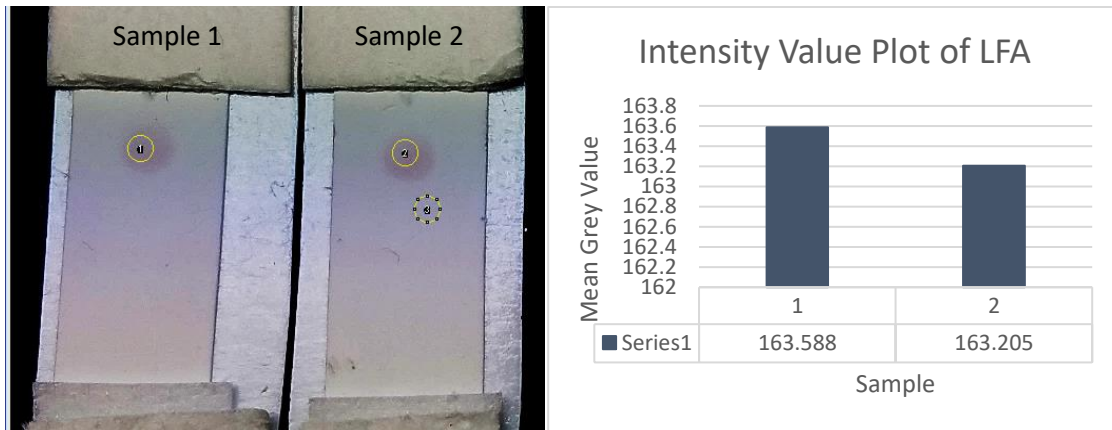
Figure 37 – ssDNA hybridization LFA spot – Mean grey value chart comparing immobilization techniques. Sample 1 corresponds to immobilization procedure of 1hr incubation at 37°C followed by overnight storage in a desiccator. Sample 2 was kept at 37°C for 2 hrs. The graph displays the mean grey values of a sample in the selected circular area in the middle of the signal location. The 1 hr at 37°C procedure displayed greater signal intensity.

membrane (Figure 36): 1) 1 hr at 37°C then overnight in the desiccator and 2) 2 hrs at 37°C then overnight in the desiccator. The whole LFA system was used for the test in order to get a baseline idea of materials needed for such tests and to display the optimal immobilization technique (results shown in Figure 37). The CO(M) was deposited into the conjugate pad as described in the conjugate pad preparation methods section, and 200 µl of 1xCOB solution was added to the sample pad which flows through the conjugate pad. Once the flow of solution reconstitutes the mobile probe, it continues through the NC membrane and a fraction is captured by the immobilized probe (Figure 38). When the CO(M) reacts with the capture ssDNA on
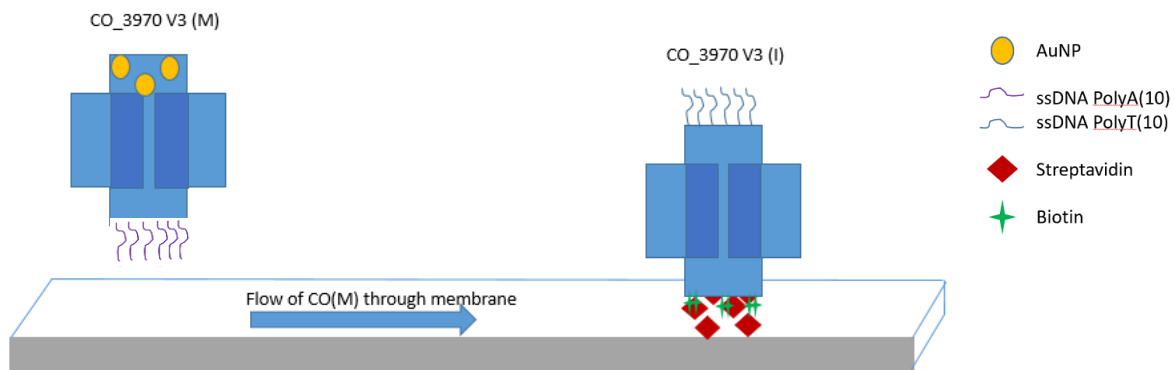
Figure 38 - Schematic of ssDNA hybridization LFA.

46

CO(I), the characteristic red line forms if enough gold-labeled material is captured. The pencil

marks label where the immobile capture probe was deposited. The result of this test was that the

red color only developed where the immobile probe was deposited.[51]
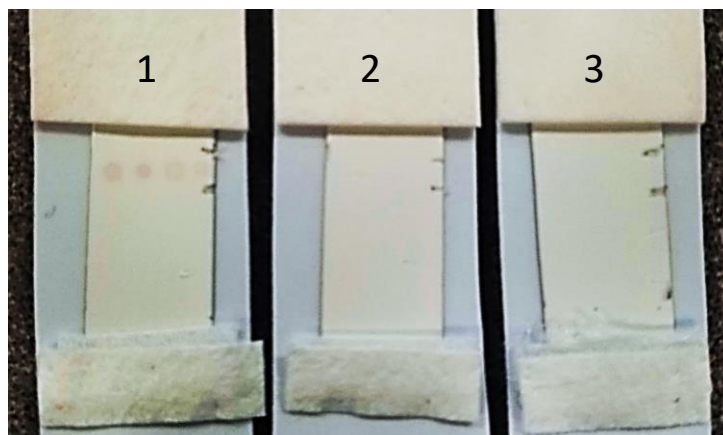
LFA	Immobile	Expected result	Observed result
1	CO(I) with 6 polyT sticky ends	+	+
2	CO(I) no sticky ends	-	-
3	Streptavidin	-	-

Figure 39 – Image of experimental control LFAs of immobile capture probe. ssDNA hybridization LFA positive vs. two negative controls. The red area between the pencil marks indicating capture occurred for the positive control and no visible line occurred in the negative control LFAs.

A second control experiment, which was mentioned in the control line preparation

methods section, examined whether there was possible interaction between the CO_3970 DNA

Origami structures, i.e., with no ssDNA extended staples available for the mobile probe to

hybridize with. A streptavidin only line was also immobilized onto the NC membrane to

examine whether binding occurred via a mobile probe-streptavidin interaction. Three membranes

were treated with either CO(I) with polyT sticky ends, CO(I) with no sticky ends or streptavidin

only (Figure 39). These negative controls were applied at the same concentration ($1.2\ \mu g/cm^2$) as

the positive control in order to maintain integrity of testing.

A high concentration (~150 nM) of both probes was used in a ssDNA hybridization

reaction LFA to try to achieve the desired 1 mg/mL or 150 nM of probe concentration (Figure
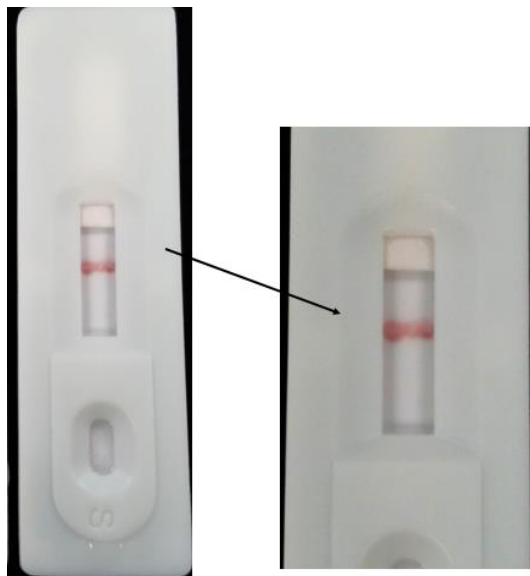
Figure 40 – Image of optimal ssDNA hybridization LFA. ssDNA hybridization LFA using higher concentrations (closer to suggested 0.5-1 mg/mL).[39] Test run and imaged in plastic casing. 6 µl of 100-200 nM DNA Origami applied to control line.

40). Testing was becoming more refined during this experiment. Deposition of the immobile

probe in three 2 µl aliquots and allowing it to dry at RT between each deposition was found to be

the best way to deposit greater quantities of probe in order to construct a well-defined control

line. The experiment showed enhanced results in intensity of the red line when compared to

previous experiments.

4.2 ANALYSIS OF TRIS-NTA COMPLEX LFA

The ability of the Tris-NTA complex incorporated into the DNA Origami to bind a His-

tagged protein was tested using AFM analysis and gel electrophoresis before an LFA experiment

was performed. Experiments to study the construct's complexation with Ni^{2+} ions and the His-

tagged fluorescent protein were conducted varying time, $NiCl_2$ concentration and protein

concentration as variables. The reaction did not produce high yields of product; however, some binding of fluorescent protein was observed (Figure 41). Initial trials were performed in DNA Origami buffer (1x TAE, 12.5 mM MgCl$_2$). A literature search into metal chelation[20] returned that EDTA enables elution of NTA-bound proteins by sequestering metal ions. All further experiments were performed in 1x Tris-acetate buffer with a high ionic concentration of NaCl to push the reaction. The highest yield was achieved when Ni^{2+} ions were preloaded onto Tris-NTA, at an NTA to Ni ratio of 1 to 10, for 30 minutes and then components (Ni^{2+} ions, CO_3970 with Tris-NTA modification and mCherry fluorescent protein) were allowed to complex over a period of 48 hours at RT. Further tests were performed in an attempt to preload Ni^{2+} ions onto

mCherry Fluorescent Protein
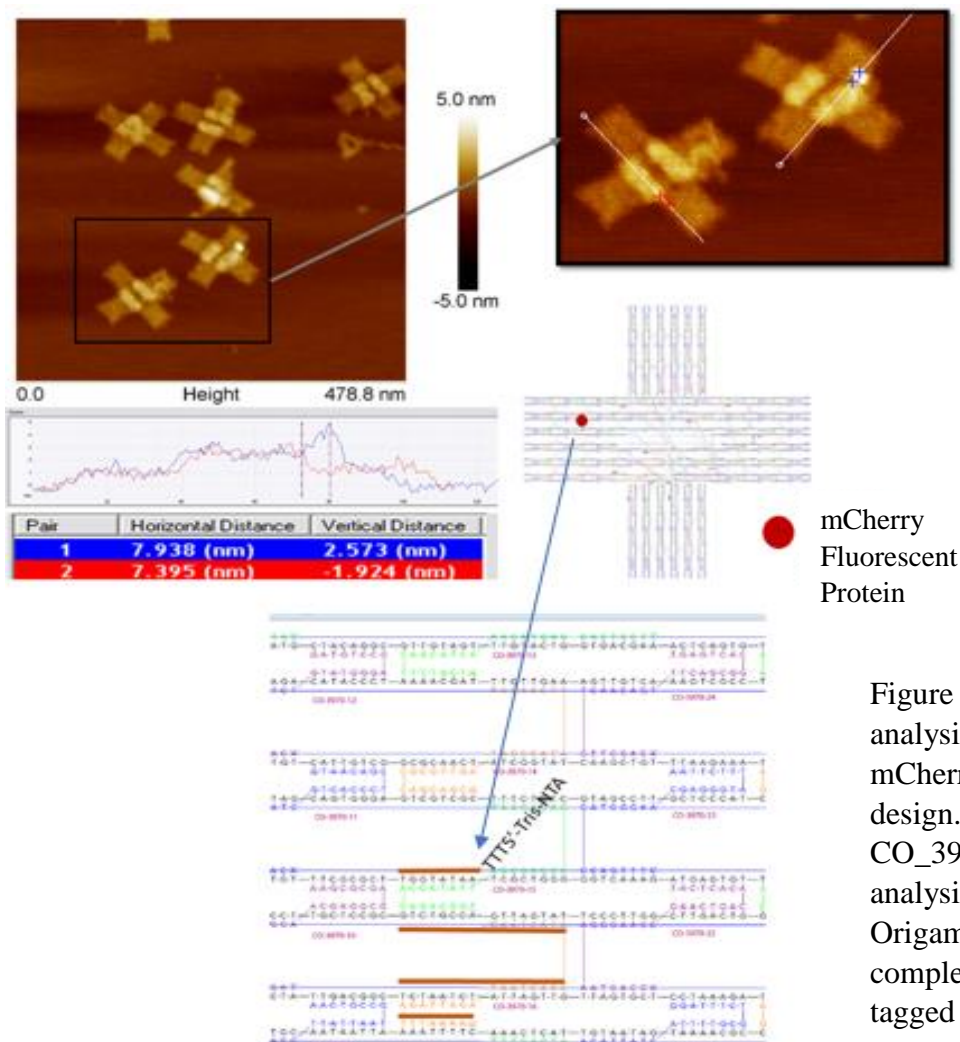
Figure 41 – AFM image and analysis of CO_NTA(I) with mCherry bound and probe design. Tris-NTA location on CO_3970, AFM images and analysis of Tris-NTA DNA Origami transition metal complexation with a His-tagged fluorescent protein.

the Tris-NTA complex and then use Sepharose column filtration (GE Gel filtration – G50) to exclude the excess Ni^{2+} ions from the solution. These steps were followed by adding the His-tagged protein and incubating for the same period of 48 hours at RT. These experiments were less successful than the first experiment, demonstrating a low yield.

A gel electrophoresis experiment was conducted in an attempt to observe an electrophoretic mobility shift when a His-tagged protein complexes with the Tris-NTA DNA staple strand (Figure 42). The staple strand alone was added to lane 3, to give a baseline and a

Lane	1	3	5	7	9	11
Contents	Ladder	Tris-NTA Staple	CO-15 half + CO-14 staple	NiCl2 w/ Tris-NTA staple	NiCl2 w/ Tris-NTA staple + dsRed FP	NiCl2 w/ Tris-NTA staple + CFP
Description	GeneRuler	ssDNA - 54 bases	ssDNA - 48 bases	Filtered – G50	Filtered G50 1hr reaction w/ protein	Filtered G50 1hr reaction w/ protein
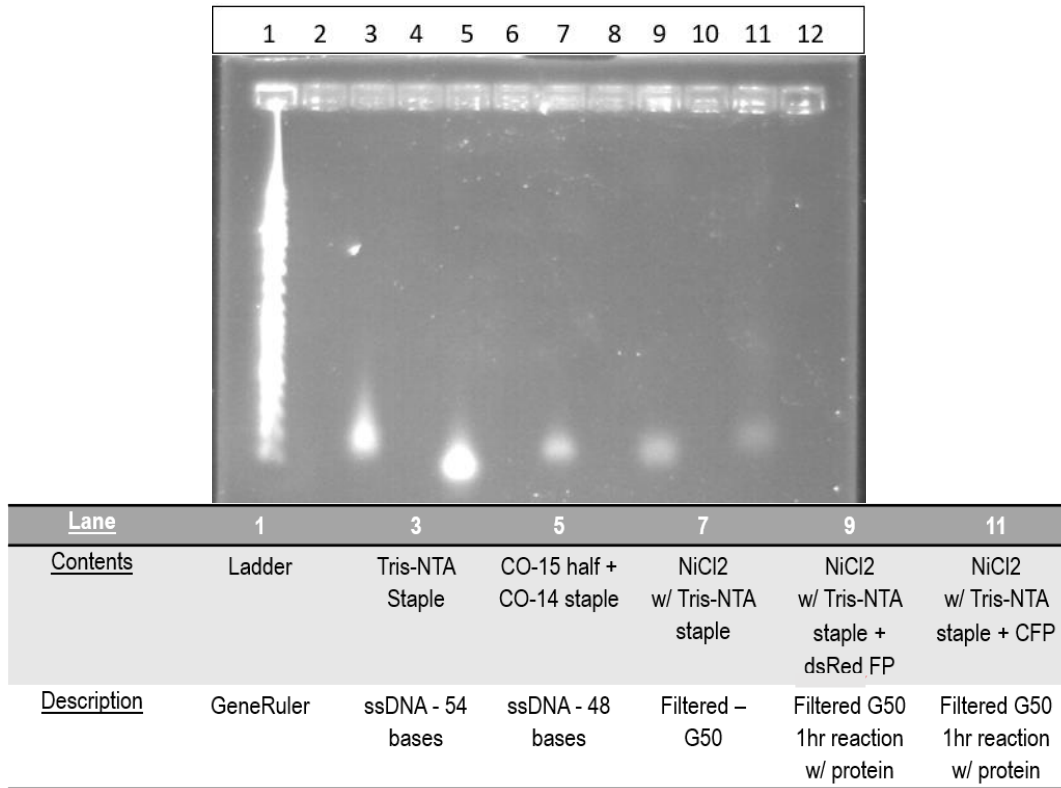
Figure 42 – EMSA gel determining complexation of NTA-Ni-His-tag. EMSA Gel – Electrophoretic mobility shift assay performed using 1.5% agarose gel to determine whether there is a detectable difference in molecular weight when protein is bound to a ssDNA staple modified with Tris-NTA in the presence of Ni^{2+} ions. G50 corresponds to the pore size in the size exclusion filter used in filtration of excess Ni^{2+} ions.

staple, which is six bases less than the NTA staple, with no modifications was run in lane 5. The

Tris-NTA staple was preloaded with Ni^{2+} ions and separated into three aliquots: one put to the

side, and the other two mixed with either dsRed fluorescent His-tagged protein or with cyan fluorescent His-tagged protein (CFP) and allowed to react for one hour. A few different His-tagged fluorescent proteins were tested to determine which, if any, His-tagged protein would participate in this reaction. The shift in lane 11 should correspond to Tris-NTA staple complexation with the His-tagged CFP. The small magnitude of the mobility shift yields an ambiguous result, perhaps consistent with a rapidly equilibrating complexation reaction.

Literature reveals that the reaction is not long lived when in solution at low concentrations with a K_D value 2.7×10^{-7} M and based on a measurement of the association rate constant for a similar construct of 10^5 $M^{-1}s^{-1}$ and a dissociation rate constant of the order of $10^{-3}s^{-1}$.[17,23] Therefore, creating an LFA using the Tris-NTA decorated DNA Origami as the immobile probe in order to capture Ni^{2+} ions relatively quickly may be more effective than the slow AFM technique (Figure 43). Using the Ni^{2+} ions as the analyte, the mobile probe would be His-tagged mCherry which would display a reporting signal by emitting photons at 610 nm when excited. A
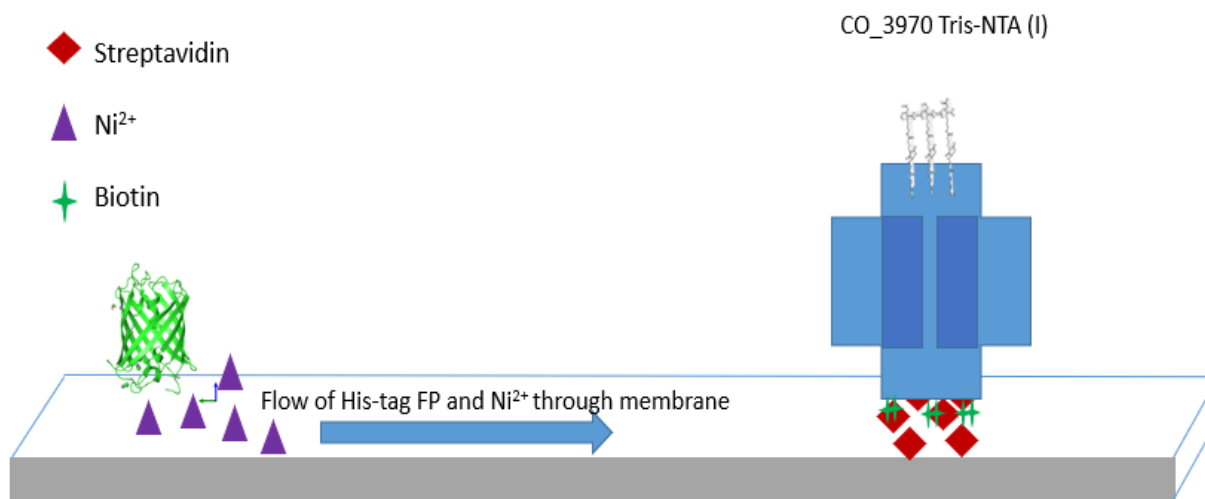
Figure 43 – Schematic of CO_NTA LFA detecting Ni^{2+} ions. Tris-NTA complexation and capture of Ni^{2+} ions and subsequent capture of the His-tagged fluorescent protein.
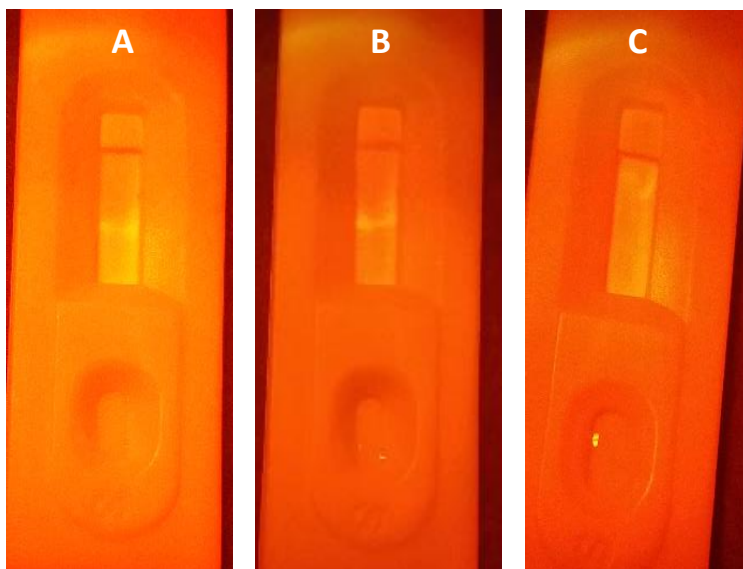
Figure 44 – Images of fluorescing mCherry in CO_NTA(I) LFA. A) Ni^{2+} ions sandwiched between mCherry fluorescent protein (reporting probe) and a Tris-NTA modification on CO_3970 (immobile probe). B) Ni^{2+} ions possibly sandwiched between mCherry fluorescent protein (reporting probe) and CO_3970 (I) with no modification (immobile probe). The line displays a positive test for Ni^{2+} ions in sample. C) Buffer-only immobilized onto the membrane assay showing no capture.

high-pressure Hg (mercury) lamp was used as the excitation source and a long pass filter was used to select the emissions from the fluorescent protein when captured at the line (Figure 44). The Ni^{2+} ions were introduced into the system in the buffer at 10X the concentration of the Tris-NTA decorated immobile probe. The completed LFA did appear to demonstrate capture of Ni^{2+} by DNA Origami structures and not from streptavidin or a buffer only control line. The immobilized Tris-NTA decorated CO-3970 showed capture and the immobilized CO_3970 without Tris-NTA also showed capture at the control line, however, no capture was observed for assays which used streptavidin or buffer-only immobilized on the membrane.

4.3 ANALYSIS OF THROMBIN BINDING APTAMER LFA

Many aptamer-based lateral flow assays have been developed over the last decade.[3] One which was successful, was specifically developed to capture Thrombin in a sandwich style using two variant DNA aptamers.[52] The same 15-mer and 29-mer DNA thrombin-binding aptamers were used for the LFA in this research. The mobile reporting probe was decorated with three 15-
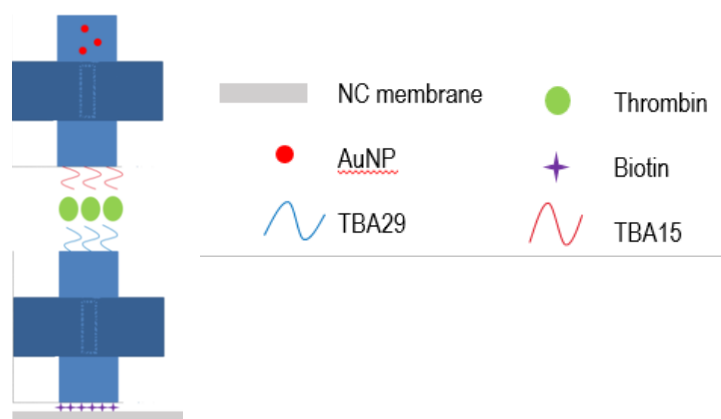
Figure 45 – Schematic of CO_TBA based LFA. Mobile reporting probe and immobile capture probe of the thrombin-binding aptamer based LFA. All modifications and elements labeled for clarification. TBA15 and TBA29 sequences in supplementary information section.
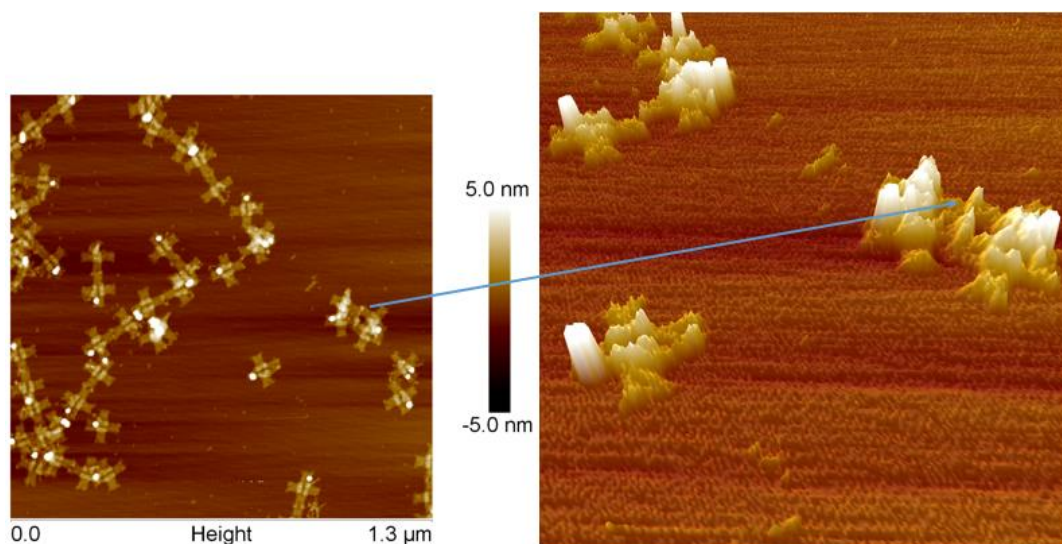
Figure 46 – AFM image of CO_TBA(M) mixed with thrombin. Left: 2D AFM image sample of gold labeled CO_TBA(M) mixed with human thrombin protein (1:10 mixed – 5min at RT). Right: 3D AFM of zoomed area of same image. Blue arrow points to thrombin sandwiched between two CO_TBA(M) constructs.

53

mer aptamer modified staples and the immobile capture probe was decorated with three 29-mer aptamer modified staples. The CO_3970 DNA Origami were then designed to accommodate these modifications and an LFA was assembled (Figure 45).

The thrombin-binding aptamer based LFA was developed using the same methods as the ssDNA hybridization based LFA and AFM images were taken of samples which were to be used in the LFA (Figure 46). However, instead of using only 1xCOB as the test sample, the buffer was also mixed with thrombin to give a final concentration of 50 nM in buffer. For the LFA

Key	Aptamer	Thrombin	Result
A	-	+	-
B	+	+	+
C	+	+	+
D	+	-	+

Figure 47 – Image of CO_TBA based LFA control experiment. Negative (A and D) and positive (B and C) control TBA LFA experiments. Successful sandwich-style capture can be seen in the positive control assay. The negative control assay which has no thrombin-binding aptamers on the immobile probe did not show a signal. Right image: Both LFAs showing capture means that thrombin-binding aptamers TBA29 and TBA15 bind to each other and give a signal.

experiments, 200 µl of this thrombin containing 1xCOB solution was run through both a positive and negative control (Figure 47). The positive control had the 29-mer thrombin aptamers on the immobile probe and the 15-mer thrombin aptamers on the mobile probe in order to capture the thrombin analyte in a sandwich-style. One negative control (Figure 47 – A) used the same

mobile probe; however the immobile probe consisted of CO_3970 with a Tris-NTA modification

as well as 6 polyT(10) sticky ends. This negative control experiment was meant to demonstrate

some specificity of the assay. The sandwiching of thrombin was observed to be successful using

the CO_3970 probes decorated with thrombin-binding aptamers (Figure 47 – B). A second

control experiment was conducted with two LFAs using thrombin-binding aptamers on all

CO_3970 DNA Origami structures. However, thrombin is introduced to one for detection, and

not the other, to test if there is any interaction between the TBAs themselves (Figure 47 – C and

D). The negative control experiment, which was absent of thrombin protein, showed a false

positive result. Upon further investigation using AFM imaging, the first version of the

CO_TBA(M) probes were shown to bind to each other via the thrombin binding aptamers in the
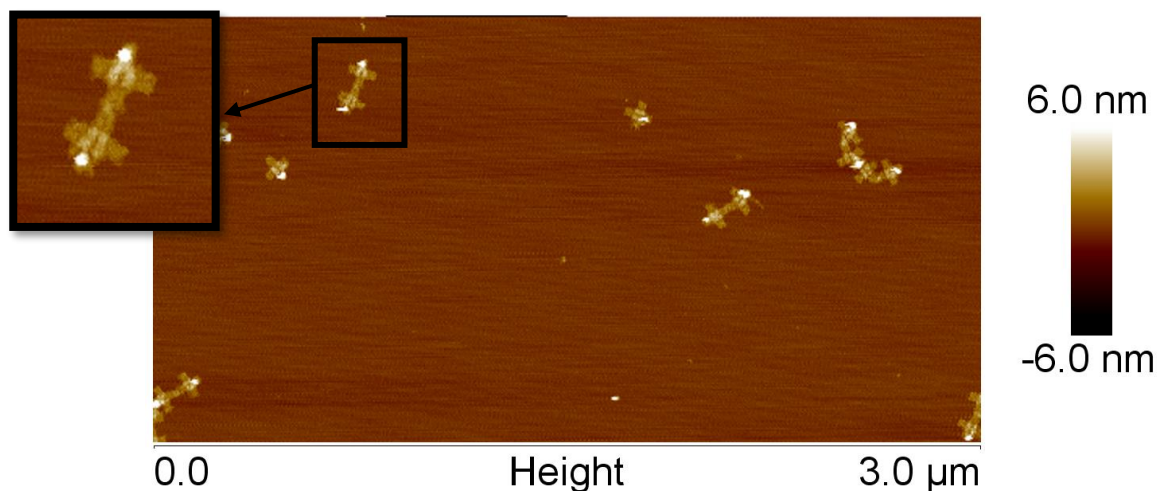
Figure 48 – AFM image of CO_TBA(M) dimerization in the absence of Thrombin. The
CO_TBA(M) with three TBA15 staple modifications dimerize to create these structures.

absence of thrombin (Figure 48). The fact that the first version of the TBAs can bind to one

another suggests that this assay is not sandwiching thrombin, but binding the immobile probe

TBA29 modifications.

The results show that the aptamers, as designed, bind to each other. Moving forward from this result, a second version of the aptamer strands was designed for the construct. The second version of the aptamers, was tethered by only the 5' end to the CO_3970, displayed binding with Thrombin which was immobilized onto a NC membrane. The test excluded the immobile probe

Figure 49 – Version 2 of CO_TBA(M) LFA. Version 2 of CO_TBA(M) tested against Thrombin immobilized onto the NC membrane. Positive capture displayed by the test.

so that the binding of one aptamer associated with the mobile probe could be concluded. The results from version 2, with only one aptamer staple on the right arm of the CO_TBA(M) probe, displayed capture at the immobilized thrombin on the membrane (Figure 49).

CHAPTER 5: DISCUSSION

5.1 CO_3970 MOBILE PROBE GOLD MODIFICATION

The sites for gold nanoparticles binding, which have extended complementary sequences on the CO_3970, were designed with precision in order to optimize the binding of up to three AuNPs onto the mobile probe construct. The sites are designed to fit the size of the 5 nm AuNP. The length added by functionalizing the AuNPs with the 10-base thiol-oligonucleotide is around 3.6 nm. The sites have three docking strands each to give sufficient specific binding consistent with the data presented in Ding et al.[35] The docking strands are also 10-bases in length because this corresponds to ~1 complete helical turn which gives better strength and stability of base pairing bonds.[5]

The design enabled efficient binding of up to three AuNPs to the CO_3970. Of the CO(M) in the AFM images (Figure 30 and 31), 99% were bound with 1 or greater than 1 AuNPs. Most constructs showed greater than 1 AuNP bound due to the 1:3 ratio of CO(M) to AuNPs. The method outlined in the conjugate pad preparation section detailed using 100 mM NaCl and annealing the mixture of CO(M) and AuNPs for 2 hours over 45-20ºC effectively accomplished the decoration of the Origami with AuNPs. Other methods, such as a longer annealing period of 4 hours were tested and shown to be unnecessary due to the efficiency of the base-pairing of only 10-base sequences.

As shown in Figure 33, the AuNPs have a height of ~5-6 nm when bound to the CO_3970. The analysis along the z coordinate of these images shows that the site-specific binding of AuNPs was accomplished in this research. The binding of inorganics to DNA Origami can allow for better visualization and confirmation of site-specific binding to DNA

Origami. If enough CO_3970 bound with AuNPs were together, moving in solution or through an LFA, one would be able to visualize this motion using the naked eye. The method is promising in that it is possible to create higher order metallic nanostructures with great precision. A control experiment was also conducted by designing an anti-sense docking strand extending from the CO_3970. The lack of observed binding displays that the binding is extremely specific for the 10-base ssDNA sequence bound to the AuNPs.

5.2 ssDNA HYBRIDIZATION LFA

Experimentation and optimization of the DNA Origami LFA primarily consisted of the basic ssDNA hybridization version of the system. The first consideration addressed was the preservation of the structures in the system. Our mixture was showcased in Figure 29 in which the DNA Origami CO_3970 structures were mixed then deposited on NC membranes. These NC membranes were dried and heated at 37^oC over 3 days and reconstituted in 1xCOB for 2 hours to demonstrate the ability of this mixture to preserve the structures. Some of the preservative mixture components, BSA and Tween20, were also used in NC membrane blocking for the lateral flow of solution through the analytical membrane so that non-specific binding does not occur during the assays (described in the Section 3: Blocking the Analytical (NC) Membrane) pg.36.

In Figures 32 and 33, the AFM images display the abilities of the two separate probes (mobile and immobile probe) to accomplish the ssDNA hybridization reaction in a relatively short amount of time. The reaction is able to be accomplished via the lateral flow of the mobile probe through the NC membrane being captured at the control line by the immobile probe. The

successful assays in Figures 36, 38 and 39 show that the mobile reporting probe is in fact being captured by the immobile probe, which enables the signal to develop. Specifically, the control experiment, shown in Figure 38, reiterates that hybridization of single stranded polyA and polyT strands is in fact the mechanism of action in these positive tests. The tests were specific and demonstrated what they were designed to show.

5.3 NTA-Ni^{2+} CHELATION AND CAPTURE OF HIS-TAGGED PROTEIN LFA

The yield and predictability of the His-tagged protein immobilization has proven to be less than expected. The excess Ni^{2+} ions may be causing difficulty because of saturation of the chelating agents (Tris-NTA and His-tag); therefore, not allowing the two agents to chelate three Ni^{2+} ions together which is required for protein immobilization. This is one possible explanation for the low yield which present studies are showing. However, exclusion of excess Ni^{2+} from the solution helped little when all components of the reaction are in solution at low concentrations.

An electrophoretic mobility shift using gel electrophoresis was performed to determine whether or not the protein complexes with the staple. The apparent visualization of a very weak shift shows that the Tris-NTA staple and His-tagged proteins do not have a long lifetime. Multiple gels were run in the hope of finding an answer to this binding problem. The gel in Figure 42 showed an apparent shift in intensity when using a cyan fluorescent protein with a His-tag. This shift indicated that the staple may be complexing with His-tagged proteins for some short time. The reaction times were also varied during this experiment and 1 hour and 24 hours displayed very similar results perhaps reflecting that the on/off reaction happens fairly quickly at room temperature.

A possible interference, when creating a sandwich LFA, is the high-dose hook effect. The high-dose hook effect can cause the analyte to interfere with reactive sites of both sandwiching probes and in turn give a false negative for the assay.[53] The effect can be avoided by dilution of sample, which was shown in the positive LFA tests. This effect could be a factor which creates false negatives when testing for Ni^{2+} capture because the ions can occupy the His-tags and the Tris-NTA and completely halt complexation. During experimentation of the Tris-NTA moiety the Ni^{2+} concentration which is added to the sample must be calculated and controlled. Other possible interferences include bond dissociation, low concentration of components, or non-specific binding of the metal ions to NC.

An LFA was created using CO_Tris-NTA as the immobile probe in order to chelate the Ni^{2+} ions which are already bound to the His-tagged fluorescent protein during travel through the assay. Using the fluorescence of the mCherry protein, the capture of the transition metal was visible using filters and an excitation source, as seen in Figure 44. The controls in this experiment were a CO(I) with polyT sticky ends with no NTA moiety, streptavidin only and buffer applied to the membrane. The CO_Tris-NTA and CO(I) with no NTA moiety both displayed capture of transition metal and signal at the line location. The reactivity of the His-tagged protein with CO(I), absent of the Tris-NTA moiety, is believed to be because of DNA Origami's negative state and ability to chelate metals in order to neutralize the charge in solution. The streptavidin and buffer only assays showed no sign of capture at the control line.

5.4 THROMBIN BINDING APTAMER LFA

The LFA designed to detect human thrombin protein did not successfully demonstrate thrombin capture due to the observation of a false positive result when thrombin was not present. The experiments which were conducted to display specific binding, at first, appeared to show binding; however, after further negative control experimentation the aptamer modified staples were found to interact with each other. The first thrombin-binding aptamer LFA was conducted with a control experiment to show specificity in Figure 46. The CO_TBA immobile probe construct was used on one analytical membrane and the CO_Tris-NTA with polyT strands on another. Both conjugate pads were dried with CO_TBA mobile probe and buffer containing thrombin was run through the system. The test seemingly displayed the successful binding of thrombin to only the immobilized TBA on the immobile probe. A control experiment demonstrated that these aptamers interact and bind with each other in the absence of thrombin in the system deeming this design of a thrombin sandwich assay unsuccessful. The LFA experiment displayed that, as designed, the first version of the thrombin binding aptamer staples can cause binding of the mobile and immobile probes in the absence of thrombin. The fact that in the absence and the presence of thrombin, two of the same CO_TBA(M) constructs dimerize (Figure 46, 48), demonstrates that the first version of the thrombin binding aptamer staples are most likely not forming correctly and causing self-dimerization.

Another LFA test which the first version of the thrombin binding aptamer staples, of CO_TBA mobile probe, were used to try to display binding to thrombin was developed. Only thrombin, streptavidin or buffer were deposited and immobilized as lines onto the NC membranes. The conjugate pads contained CO_TBA mobile probe and 1xCOB flowed through the system. No positive result was recorded which further illustrates that non-specific binding

61

occurs between the aptamers because there was no recorded positive result for the immobilized thrombin protein.

The lack of a positive control for binding Thrombin by the first version of the CO probes with aptamers prompted the design of a second version of probes. The modified staple strands which contained the aptamer sequence were changed in the second version to only tether from one side of the 3D G-quad structure. The first version had some constraint of the structure involved with trying to tether both the 5' and 3' ends into the Origami. This second version design of the probe displayed binding with Thrombin with no detection of aptamers dimerizing and binding to each other via AFM images.

CHAPTER 6: CONCLUSIONS

The DNA Origami designs created for this research do in fact allow for site-specific immobilization of many modifications in order to create specific structures to mimic antibodies in LFAs. The DNA Origami constructs were compatible with all of the LFA components. The LFAs tested all appeared to display and signal the capture of the species in question whether it was ssDNA hybridization, NTA chelation of a transition metal or the use of TBAs to bind to thrombin. The fact that these solid structures are reconfigurable, and able to be manipulated at will, allows for changes in modifications of probe structures over a one-day period if modifications are in hand. These structures have potential for use for hybridizing with viral or bacterial DNA/RNA, sensing a transition metal and use with DNA based aptamers for protein detection with further refinement.

The AuNPs bind extremely well to the modified CO_3970. The yield for this experiment was very high and shows site-specificity. The fact that the anti-sense docking strands did not enable binding shows that the docking sites must be sequence specific and 10 base pairing is enough for specific binding. The fact that a solid structure can be created for signaling and can be modified without disturbing the signaling system, shows that a single probe design will work for many applications. The only modification to the CO mobile reporting probe during the ssDNA hybridization and TBA experiments was to the terminal sticky ends of the construct. All other parts of the probe were the same showing the wide applicability of these designed probes.

CHAPTER 7: ADDITIONAL WORK

7.1 LYOPHILIZATION OF DNA ORIGAMI

The ability to preserve and concentrate the DNA Origami for use on a larger scale became a question relevant for its uses in an LFA product. An experiment was conducted to lyophilize and store DNA Origami while trying to optimize the possible probe concentration and storage process if DNA Origami LFAs were to be commercially produced. Lyophilization is a
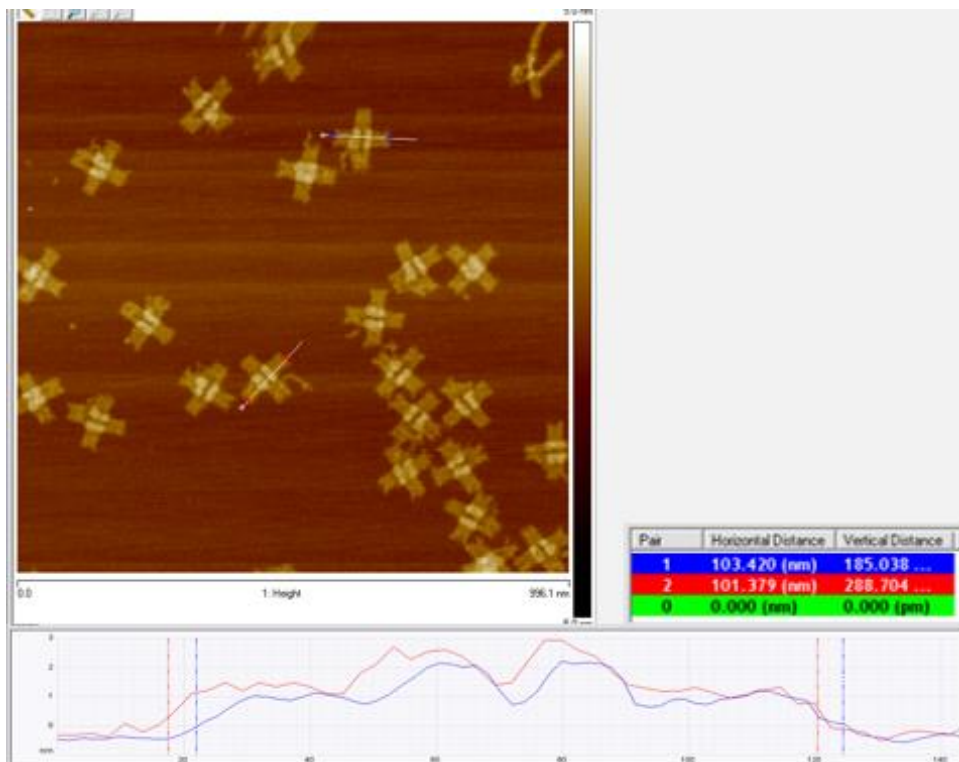
Figure 50 – AFM images and analysis of reconstituted lyophilized DNA. Analysis of the structures shows that they are the average size (100 nm) for the cross-shaped Origami and appear to be well-formed even after the freeze-drying process.

freeze-drying process where water is removed from the product. The process allows for a specific number of DNA Origami to be dried in a container and to be hydrated to a specific concentration when needed.

The experiment begins with freezing a solution of purified DNA Origami of known concentration (50 nM) under -80ºC conditions. Once the solution is completely frozen, it is then hurriedly placed in a vacuum system and allowed to dehydrate. The system reached 35 mtorr over 1.5 hours and the solution had evaporated and the dried DNA was somewhat visible in the bottom of the tube as a white flaky substance. The tube was closed immediately and placed in the -15ºC freezer. After 7 days the solution was rehydrated to a specific higher concentration (200 nM) and imaged (Figure 50). The AFM image shows that lyophilization is a viable option for storage and concentration of the DNA Origami probes used for LFA devices.

7.2 AuNP CONCENTRATION EXPERIMENTS FOR VISUALIZATION

Concentration of AuNPs at the control line gives the indication signal necessary for determination of a positive or negative assay. To complete the assays the number of

Line #	Volume (uL)	Concentration	Area (mm^2)	Moles	Particles/mm^2
1	4	81nM	18	3.2E-13	1.1E10
2	4	160nM	18	7.5E-13	2.5E10
3	4	250nM	18	10E-13	3.3E10
4	4	550nM	18	2.2E-12	7.4E10
5	4	1050nM	18	4.1E-12	1.4E11

Figure 51 – AuNP values on NC membrane to facilitate visualization. NC with different amounts of AuNPs dried onto the surface. The line number pictured from top to bottom. Line one is as supplied and line 5 was the pellet after centrifugation for 90min at 20000 RPC (14000 RPM). Lines 2-4 are dilutions of the AuNP pellet. Table includes the volume added, area occupied, moles and nanoparticles per millimeter^2.

nanoparticles necessary for visualization needed to be determined. Concentrating a solution of AuNP and depositing the solution on a NC membrane was necessary to determine the signal intensity if 100% probe binding was achieved. Different dilutions of AuNP solutions were deposited on the membrane to display the signals of nanoparticles per millimeter^2 (Figure 51).

7.3 STREPTAVIDIN-NC MEMBRANE BINDING CHARACTERIZATION

EXPERIMENT USING FLUORESCENCE MAPPING AND SPECTROSCOPY

A control experiment demonstrates that optimal binding is not achieved without pre-incubation of streptavidin with the biotinylated probe. The confocal (Leica) was used to show what lateral flow of 1xCOB through the membrane does to a non-immobilized probe. The
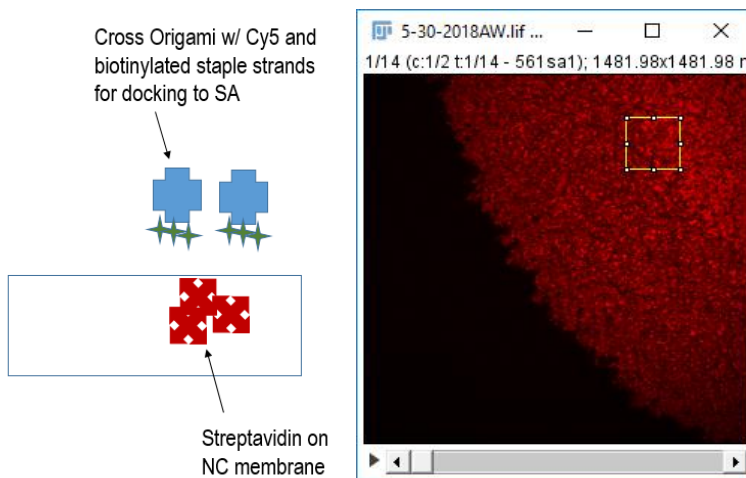
Figure 52 – Immobilization experiment schematic and Confocal images. Left: Immobilization experiment schematic showing streptavidin and CO(I) with different fluorophores attached. Right: Imaging an area of deposition using the confocal microscope. The different excitation and emission wavelengths of Cy3 (561 nm and 575 nm) and Cy5 (633 nm and 665 nm) allow for separate quantification using Confocal microscopy.

streptavidin and biotinylated immobile probe were equipped with fluorophores (Cy3 and Cy5) for visualization (SA-Cy3 - Life Technologies) (Cy5 decorated staple for CO(I) probe – IDT). Streptavidin with Cy3 and the biotinylated immobile probe with Cy5. The streptavidin with Cy3 was spotted (1 µl of either 1.5 mg/ml or 1% of that 0.015 mg/ml) on the membrane and allowed to dry for 1 hour in a vacuum chamber. After drying the streptavidin, the CO immobile probe with Cy5 was spotted (2 µl of 100 nM solution) directly on top of the dried streptavidin spot on the membrane and allowed to dry in vacuum chamber for 1 hour (Figure 52 - left). After drying the deposition spots were imaged using a Leica Confocal with the 633 nm laser to excite the Cy5

on the CO immobile probe to get a value before 1xCOB was laterally flowed through the

membrane (Figure 52 - right). After lateral flow of buffer through the membrane the depositions
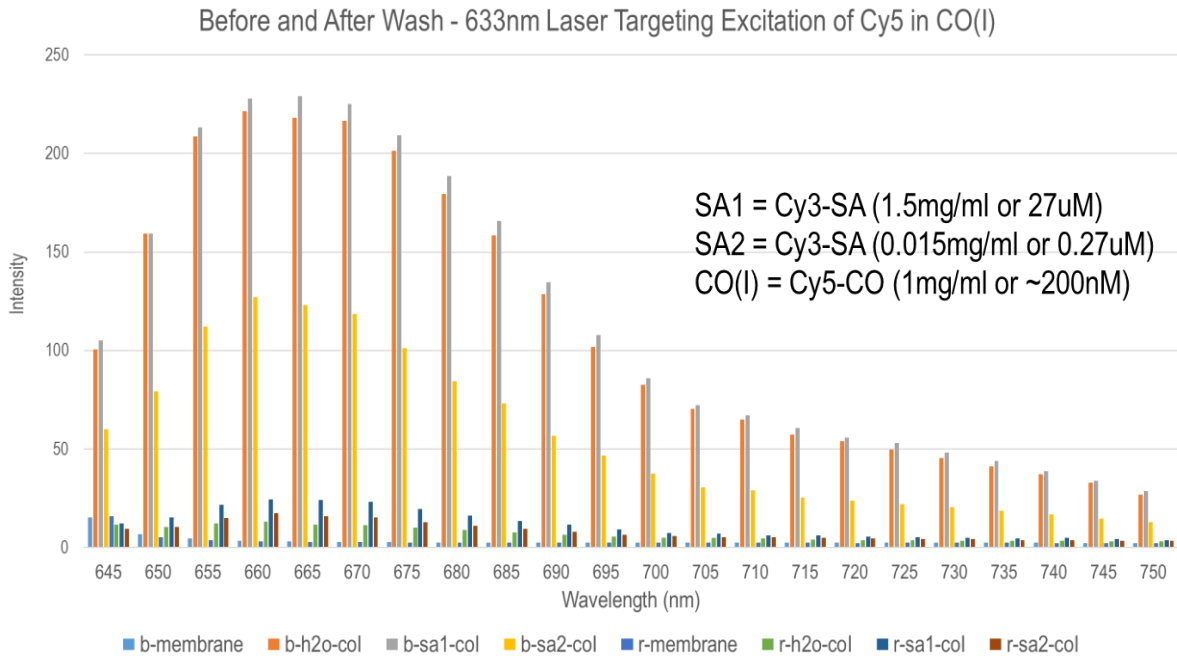
Figure 53 – Graphic chart representing the relative intensities of the fluorophores before and after lateral flow of buffer through the system. The before rehydration intensities are designated with a **b-** and the rehydrated (buffer laterally flowed through system) images are designated with an **r-**. Water or two concentrations of streptavidin were immobilized on the membrane and CO(I) was deposited onto the same place. The after images are significantly lower showing that the CO(I) were not immobilized to the membrane via streptavidin with only 1hr drying in a vacuum chamber. More information about microscope parameters in supplementary information.

were imaged again and decreased values for Cy5 from the CO immobile probe were significant

(~1/10 of the original signal) (Figure 53). The decrease in value after dry interaction between the

biotinylated probe and streptavidin only further reinforced the need for pre-incubation of these

two species before immobilization on the membrane.

7.4 ZIKA VIRUS GENOME ssDNA HYBRIDIZATION LFA

An LFA was designed to demonstrate the ability of the Cross Origami probes to be modified to suit many functions. The Zika Virus LFA displays that the staples can be modified to protrude from the arms in order to capture and hybridize with a specific ssDNA sequence. In this
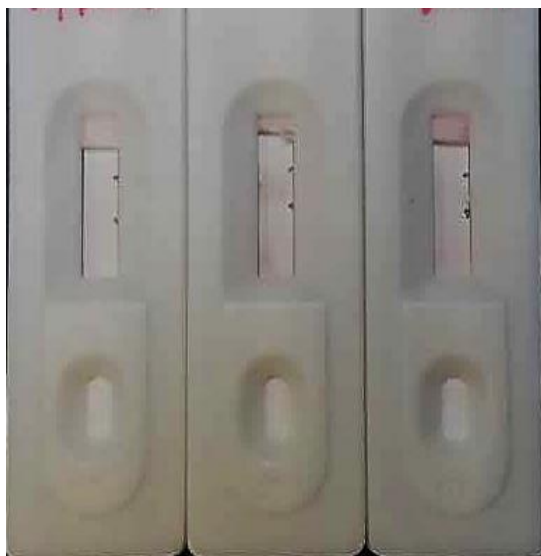
Control	Negative	Positive	Negative
CO_ZKV(M)	+	+	+
CO_ZKV(I)	-	+	+
ZKV ssDNA sequence	+	+	-

Figure 54 – Image of detection of a ssDNA Zika Virus sequence using concept of ssDNA hybridization LFA. Detection of ssDNA Zika Virus sequence using DNA Origami probes in a complete LFA system. Table displays contents of the positive and two negative controls tested.

case, part of the Zika Virus genome was selected (from NCBI) to show that detection of specific DNA sequences is possible using these DNA Origami probes. The probe designs and genomic sequence were selected with rate constants in mind. The rate at which dissociation occurs or k_{off} is strongly dependent on the length of the duplex formed by docking strands (k_{off}) 1.6 s^{-1} for 9 bp

and 0.2 s^{-1} for 10 bp, while k_{on} is only weakly dependent on this length.[54] Therefore, 15base-pairing per probe should suffice to achieve a signal.

One such example shows that, when the specific ssDNA Zika Virus genome sequence is added during sample deposition, a positive result occurs when the CO(M) and CO(I) probes are equipped with protruding detection ssDNA strands complementary to an oligomer with a specific Zika Virus sequence (Figure 54). Two negative controls were also tested to ensure that this was a true positive control. One consisted of immobilized CO(I) with no Zika Virus complementary sequences and the only modification was biotinylation of the right arm. The other negative control consisted of both CO_ZKV probes, however, no ssDNA Zika Virus genome sequence was added to the sample. All LFAs in this test had CO_ZKV(M) probe in the conjugate pad.

Author Contributions

Adrienne Walker (AW), David Neff (DN) and Michael L. Norton (MLN) conceived and designed the experiments. AW performed the experiments. AW and MLN analyzed the data.

Conflicts of Interest

The authors declare no conflict of interest. The funding sponsors had no role in the design of the study; in the collection, analyses, or interpretation of the manuscript and in the publication of the results.

Supplementary Information

Modified staple strands for three AuNP binding

CO-3970-half12and1-v3AW	GTATGGGAGCCTGTAGCATTCCACAGACAGCCCTCATAGTCAGACGTT
CO-3970-2andhalf3-v3AW	AGTAAATGCATCGCCCACGCATAAGTTAAAGGCCGCTTTTCAACGGAG
CO-3970-half3andhalf4-v3AWaunp	AGGGAAGAACTTTATTTGTATCCTGCTCCATGTTACTACATTTGA
CO-3970-half4and5-v3AW	GGATTTAGCGTATTAAATCCTTTGTTTTCAGGTTTAACGTTCGGGAGA
CO-3970-9andhalf10-v3AW	TGCGTAGACCCGAACGTTATTAATGCCGTCAATAGATAATTAGCCGGA
CO-3970-half10andhalf11-v3AWaunp	AGGGAAGAACTTTACGAGGCGAGCGCGAAACAAAGTAGCGGGATC
CO-3970-half11andhalf12-v3AWaunp	AGGGAAGAACTTTGTCACCCTCGACAATGACAACAACAATTTTCT
CO-3970-half22half23-v3AW	GAACTGACACACTCATCTTTGACCCATCGGAA
CO-3970-half23half24-v3AWaunp	AGGGAAGAACTTTCGAGGGTATTTCTTAAACAGCTTGTCAACAGT

70

CO-3970-half24and13-v3AWaunp	AGGGAAGAACTTTTTCAGCGGCACTGAGTTTCGTCACCAGTACAA
CO-3970-half13and14-v3AW	ACTACAACTTTTGCTAAACAACTTATACCGATAGTTGCGCCAGCAGCG
CO-3970-short25-v3AW	CCAATAGGAACCCATGTACCGTAAAGT
CO-3970-some25and26-v3AWaunp	AGGGAAGAACTTTGAGAATAGAAAGGTTGCTTTCGAGGTGAAGCAACGGC
CO-3970-16andhalf17-v3AW	CAATCATACAACTAATAGATTAGATTTAAAAGTTTGAGTACACGTAAA
CO-3970-half17andhalf18-v3AWaunp	AGGGAAGAACTTTACAGAAATCTTTGAATACCAAGTTCCTTGCTT
CO-3970-half18andhalf19-v3AW	CTGTAAATCATAGGTCTGAGAGACTACCTTTT
CO-3970-half19andhalf20-v3AW	TAACCTCCATATGTGAGTGAATAAACAAAATC
CO-3970-half20andhalf21-v3AWaunp	AGGGAAGAACTTTGCGCAGAGATATCAAAATTATTTGACATTATC
CO-3970-half21andhalf22-v3AWaunp	AGGGAAGAACTTTATTTTGCGTCTTTAGGAGCACTAAAGGGAACC

AuNP complementary sequences labeled in black. Different colors denote different sections of original staple sequences incorporated into the newly designed staples.

Thiol-oligonucleotide sequence for functionalization of AuNP

5' GTTCTTCCCT/3ThioMC3-D/

Modified Tris-NTA staple strand

CO-3970-15- NTA-5'(TTT) Elongated 15-16)	Tris-NTA 5' - TTTTTATACCACAGACGGTCAATCATACAACTAATAGATTAGATTTAAAAG
CO-3970-15 Short Elongated 14-15	AACAACTTATACCGATAGTTGCGCCAGCAGCGAAAGACAGCCCAGCGA

Version 1 of the Thrombin-binding aptamer sequences

CO-3970-R1 CO(M)TBA15 (T10)	CATCGATAGGCCGGAATTTTTTTTTT**GGTTGGTGTGGTTG G**TTTTTTTTTTTACGTCACCAATGAAAC
CO-3970-R3 CO(M)TBA15 (T10)	AAACAGGGGCCTTTACTTTTTTTTTT**GGTTGGTGTGGTTGG** TTTTTTTTTTAGAGAGAATAACATAA
CO-3970-R5 CO(M)TBA15 (T10)	ATCGGCTGCGAGCATGTTTTTTTTTT**GGTTGGTGTGGTTGG** TTTTTTTTTTAGAAACCAATCAATA
CO-3970-L1 CO(I)TBA29 (T10)	CGTCTTTCTAGCGTAATTTTTTTTTT**AGTCCGTGGTAGGGC AGGTTGGGGTGACT**TTTTTTTTTTCGATCTAAAGTTTTGT
CO-3970-L3 CO(I)TBA29 (T10)	ATCCGCGACATCGCCTTTTTTTTTT**AGTCCGTGGTAGGGC AGGTTGGGGTGACT**TTTTTTTTTTGATAAATTGTGTCGAA
CO-3970-L5 CO(I)TBA29 (T10)	CTTTTACACAGATGAATTTTTTTTTT**AGTCCGTGGTAGGGC AGGTTGGGGTGACT**TTTTTTTTTTTATACTAGTAACAGTAC

Bolded sections denote Thrombin-binding aptamer sequences which fold into g-quad structures.

Immobilization Experiment: Confocal

Leica Confocal settings and additional information regarding immobilization experiment.

	paper	Streptavidin (1.5mg/ml ~27uM – Cy3 conjugated)	Streptavidin (0.015mg/ml ~0.27uM – Cy3 conjugated)	H2O MilliQ
Volume added	-	1ul	1ul	1ul
CO(I) ~200nM	-	x	X	x
Laser Used (nm)	405, 561, 633	405, 561, 633	405, 561, 633	405, 561, 633
X,y lambda (change in wavelength over 5nm increments)	405= 420-650nm 561= 575-650nm 633= 645-750nm	405= 420-650nm 561= 575-650nm 633= 645-750nm	405= 420-650nm 561= 575-650nm 633= 645-750nm	405= 420-650nm 561= 575-650nm 633= 645-750nm
Laser strength (%)	20	20	20	20
Before wash image	B-paper	B-sa1-col	B-sa2-col	B-h2o-col
Washed (5min in COB1x – agitated every minute) image	R-paper	R-sa1-col	R-sa2-col	R-h2o-col

Cy5 CO_3970 staples for Confocal Immobilization Experiment

CO-3970-3 5'(Cy5)(I)-AW ISD3	/5Cy5/TT TAT TTG TAT CCT GCT CC
CO-3970-17 5'(Cy5)(I)-AW ISD3	/5Cy5/TT TAC AGA AAT CTT TGA AT
CO-3970-24 5'(Cy5)(I)-AW ISD3	/5Cy5/TT TTT CAG CGG CAC TGA GT

ssDNA hybridization LFA CO_3970: polyA staples for CO(M), polyT and biotinylated staples for CO(I)

CO-3970-R1 MR1 (M)(5'-A10)   AAAAAAAAAA -AATGAAACCATCGATAGGCCGGAAACGTCACC
CO-3970-R2 MR1 (M)(5'-A10)   AAAAAAAAAA -GTTAGCAAACGTAGAACCTTATTACGCAGTAT
CO-3970-R3 MR1 (M)(5'-A10)   AAAAAAAAAA -TAACATAAAAACAGGGGCCTTTACAGAGAGAA
CO-3970-R4 MR1 (M)(5'-A10)   AAAAAAAAAA -TTCCAGAGCCTAATTTACGCTAACGAGCGTCT
CO-3970-R5 MR1 (M)(5'-A10)   AAAAAAAAAA -AATCAATAATCGGCTGCGAGCATGTAGAAACC
CO-3970-R6 MR1 (M)(5'-A10)   AAAAAAAAAA -TATCATATGCGTTATAGAAAAAGCCTGTTTAG

CO-3970-L1 MR1 (I)(5'-T10)   TTTTTTTTTT -AGTTTTGTCGTCTTTCTAGCGTAACGATCTAA
CO-3970-L2 MR1 (I)(5'-T10)   TTTTTTTTTT -CTGAGGCTTGCAGGGACCGATATATTCGGTCG
CO-3970-L3 MR1 (I)(5'-T10)   TTTTTTTTTT -GTGTCGAAATCCGCGACATCGCCTGATAAATT
CO-3970-L4 MR1 (I)(5'-T10)   TTTTTTTTTT -AAACAATTCGACAACTAAGTATTAGACTTTAC
CO-3970-L5 MR1 (I)(5'-T10)   TTTTTTTTTT -AACAGTACCTTTTACACAGATGAATATACAGT
CO-3970-L6 MR1 (I)(5'-T10)   TTTTTTTTTT -AGCTTAGATTAAGACGTTGAAAACATAGCGAT

CO-3970-R4 MR1 (I)(5′3'Biotin)   /5'Biotin/TTCCAGAGCCTAATTTACGCTAACGAGCGTCT/3'Biotin
CO-3970-R2 MR1 (I)(5'3′Biotin)   /5'Biotin/GTTAGCAAACGTAGAACCTTATTACGCAGTAT/3'Biotin
CO-3970-R6 MR1 (I)(5'3′Biotin)   /5'Biotin/TATCATATGCGTTATAGAAAAAGCCTGTTTAG/3'Biotin

ssDNA hybridization LFA CO_3970: Zika Virus Genomic strand staple, ZKV hybridization staples for CO(I) and CO(M)

ZKV ssDNA genomic H. Sapiens
/5ATTO647NN/TC AAT GCT AGG AAG GAG AAG AAG AGA CGA G

CO_ZKV(M) V2 - right arm
CO-3970-R1 V2 CO(M)ZKV   C CTT CCT AGC ATT GA - AATGAAACCATCGATAGGCCGGAAACGTCACC
CO-3970-R3 V2 CO(M)ZKV   C CTT CCT AGC ATT GA - TAACATAAAAACAGGGGCCTTTACAGAGAGAA
CO-3970-R5 V2 CO(M)ZKV   C CTT CCT AGC ATT GA - AATCAATAATCGGCTGCGAGCATGTAGAAACC

CO_ZKV(I) V2 - left arm

CO-3970-L1 V2 CO(I)ZKV	AGTTTTGTCGTCTTTCTAGCGTAACGATCTAA -	C TCG TCT CTT CTT CT
CO-3970-L3 V2 CO(I)ZKV	GTGTCGAAATCCGCGACATCGCCTGATAAATT -	C TCG TCT CTT CTT CT
CO-3970-L5 V2 CO(I)ZKV	AACAGTACCTTTTACACAGATGAATATACAGT -	C TCG TCT CTT CTT CT

Sequences complementary to the Zika Virus Genomic strand are labelled in blue.

Version 2 design of Thrombin Binding Aptamer LFA CO_3970: staples for CO(I) and CO(M)

VERSION 2	Open 5' end of aptamer
CO-3970-R1 V2-COTBA15(M)(T10)	**GGTTGGTGTGGTTGG**TTTTTTTTTTTAATGAAACCATCGATAGGCCGGAAACGTCACC
CO-3970-R3 V2-COTBA15(M)(T10)	**GGTTGGTGTGGTTGG**TTTTTTTTTTTAACATAAAAACAGGGGCCTTTACAGAGAGAA
CO-3970-R5 V2-COTBA15(M)(T10)	**GGTTGGTGTGGTTGG**TTTTTTTTTTTAATCAATAATCGGCTGCGAGCATGTAGAAACC
CO-3970-L1 V2-COTBA29(I)(T10)	**AGTCCGTGGTAGGGCAGGTTGGGGTGACT**TTTTTTTTTTTAGTTTTGTCGTCTTTCTAGCGTAACGATCTAA
CO-3970-L3 V2-COTBA29(I)(T10)	**AGTCCGTGGTAGGGCAGGTTGGGGTGACT**TTTTTTTTTTTGTGTCGAAATCCGCGACATCGCCTGATAAATT
CO-3970-L5 V2-COTBA29(I)(T10)	**AGTCCGTGGTAGGGCAGGTTGGGGTGACT**TTTTTTTTTTTAACAGTACCTTTTACACAGATGAATATACAGT

REFERENCES

1. G. Posthuma-Trumpie, J. Korf and A. Amerongen, *Lateral flow (immuno)assay: its strengths, weaknesses, opportunities and threats. A literature survey.* Anal Bioanal Chem, 2009. **393**: 569-582.

2. S.A Butler, S.A Khanlian and L.A Cole, *Detection of early pregnancy forms of human chorionic gonadotropin by home pregnancy test devices.* Clinical Chemistry, 2001. **47**: 2131-2136.

3. A. Chen, S. Yang, *Replacing antibodies with aptamers in lateral flow immunoassay.* Biosensors and Bioelectronics 2015. **71**: 230-242.

4. Bangs Laboratories, Inc. (1999). Lateral Flow Tests.

5. P. Rothemund, *Folding DNA to create nanoscale shapes and patterns.* Nature, 2006. **440**: 297-302.

6. W. Liu, H. Zhong, R. Wang, and N. Seeman. Crystalline Two-Dimensional DNA Origami Arrays. Angew Chem Int Ed Engl, 2011. **50(1)**: 264–267.

7. A. Keller, I. Bald. *Molecular Processes Studied at a Single-Molecule Level Using DNA Origami Nanostructures and Atomic Force Microscopy.* Molecules, 2014. **19**: 13803-13823.

8. C. Steinghauer, R.Jungmann, T. Sobey, F. Simmel and P. Tinnefeld, *DNA Origami as a Nanoscopic Ruler for Super-Resolution Microscopy.* Angewandte Chemie, 2009. **48**: 8870-8873.

9. J. Zenk, C. Tuntivate, and R. Schulman, *Kinetics and Thermodynamics of Watson-Crick Base Pairing Driven DNA Origami Dimerization.* J. Am. Chem. Soc., 2016. **138**: 3346-3354.

10. N. Voigt, T. Tørring, A. Rotaru, M. Jacobsen, J. Ravnsbæk, R. Subramani, W. Mamdouh, J. Kjems, A. Mokhir, F. Besenbacher and K. Gothelf. Single-molecule chemical reactions on DNA origami. Nature Nanotechnology, 2010. **5**: 200-203.

11. H. Erickson, *Size and Shape of Protein Molecules at the Nanometer Level Determined by Sedimentation, Gel Filtration, and Electron Microscopy.* Biological Procedures Online, 2009. **11(1)**: 32-51.

12. J. SantaLucia, H. Allawi and P. Seneviratne, *Improved Nearest-Neighbor Parameters for Predicting DNA Duplex Stability.* Biochemistry, 1996. **35**: 3555-3562.

13. B. Rohrman, E. Molyneux and R. Richards-Kortum, *A Lateral Flow Assay for Quantitative Detection of Amplified HIV-1 RNA.* PLOS ONE, 2012. **7(9)**: 1-8.

75

14. A. Baeumner, K. Edwards, *Optimization of DNA-tagged dye-encapsulating liposomes for lateral-flow assays based on sandwich hybridization.* Analytical Bioanalytical Chemistry, 2006. **386**: 1335-1343.

15. C. Liu, C. Yeung, P. Chen, M. Yeh and S. Hou, *Salmonella detection using 16S ribosomal DNA/RNA probe-gold nanopatricles and lateral flow immunoassay.* Food Chemistry, 2013. **141**: 2526-2532.

16. M. Jauset-Rubio, T. Mairal, C. McNeil, N. Keegan, A. Saeed, M. Abbas, M. El-Shahawi, A. Bashammakh, A. Alyoubi and C. O'Sullivan, *Ultrasensitive, rapid and inexpensive detection of DNA using paper based lateral flow assay.* Scientific Reports, 2016. **6**: 37732-37742.

17. C. Goodman, J. Malo, W. Ho, M. McKee, A. Kapanidis and A. Turberfield, *A Facile Method for Reversibly Linking a Recombinant Protein to DNA.* ChemBioChem, 2009. **10**: 1551-1557.

18. W. Kirk, *Thermodynamics of imidazole-ligand binding to Ni-nitrilotriacetate in solution and covalently attached to agarose beads: Imidazole, his-6 (his-tag) peptide and a new bis-imidazolo-dithiane.* Protein Expression and Purification, 2014. **95**: 1-7.

19. W. Shen, D. Neff and M. Norton, *NTA Directed Protein Nanopatterning on DNA Origami Nanoconstructs.* Journal of the American Chemical Society, 2009. **131**: 6660-6661.

20. Company, G.E., *HiTrap affinity columns: HisTrap FF*, in *GE Healthcare*. 2004: Sweden.

21. S. Lata, R. Brock, R. Tampé and J. Piehler, *High-affinity adapters for switchable recognition of histidine-tagged proteins.* J. Am. Chem. Soc., 2005. **127(29)**: 10205-10215.

22. C. Piehler, C.You, *Multivalent chelators for spatially and temporally controlled protein functionalization.* Analytical Bioanalytical Chemistry, 2014. **406**: 3345-3357.

23. R. Valiokas, G. Klenkar, A. Tinazli, A. Reichel, R. Tampe, J. Piehler, B. Liedberg, *Self-Assembled Monolayers Containing Terminal Mono-, Bis-, and Tris-nitrilotriacetic Acid Groups: Characterization and Application.* Langmuir, 2008. **24(9)**: 4959-4967.

24. A. Ellington, J. Szostak., *In vitro selection of RNA molecules that bind specific ligands.* Nature, 1990. **346**: 818-822.

25. S. Gopinath, *Methods developed for SELEX.* Anal Bioanal Chem, 2007. **387**(1): 171-182.

26. S. Rinker, Y. Liu, R. Chhabra and H. Yan, *Self-assembled DNA nanostructures for distance-dependant multivalent ligand-protein binding.* Nature Nanotechnology, 2008. **3**: 418-422.

27. C. Lin, Y. Liu, J. Zhang and H. Yan, *Self-Assembled Signaling Aptamer DNA Arrays for Protein Detection.* Angewandte Chemie, 2006. **118**: 5422-5427.

28. A. Rangnekar, S. Li, K. Bompiani, M. Hansen, K. Gothelf, B. Sullenger and T. LaBean, *Increased anticoagulant activity of thrombin-binding DNA aptamers by nanoscale organization on DNA nanostructures.* Nanomedicine, 2012. **8**: 673-681.

29. E. Katilius, Z. Katiliene, N. Woodbury, *Signaling Aptamers Created Using Fluorescent Nucleotide Analogues.* Anal. Chem., 2006. **78**: 6484-6489.

30. R. Chhabra, J. Sharma, Y. Ke, Y. Liu, S. Rinker. S. Lindsay and H. Yan, *Spatially Addressable Multiprotein Nanoarrays Templated by Aptamer-Tagged DNA Nanoarchitectures.* J. Am. Chem. Soc., 2007. **129**: 10304-10305.

31. C. Mirkin, R. Letsinger, R. Mucic and J. Storhoff, *A DNA-based method for rationally assembling nanoparticles into macroscopic materials.* Nature, 1996. **382**: 607-609.

32. A. Alivisatos, K. Johnsson, X. Peng, T. Wilson, C. Loweth, M. Bruchez, P. Schultz, *Organization of 'nanocrystal molecules' using DNA.* Nature 1996, **382**: 609-611.

33. A. George, R.Ye, L. Zhuang, X. Yang, Z. Shen and M. Zhou, *DNA Origami Site-Specific Arrangement of Gold Nanoparticles.* NanoLetters, 2013. **8(6)**: 1-11.

34. Q. Liu, C. Song, Z. Wang, N. Li and B. Ding, *Precise organization of metal nanoparticles on DNA origami template.* Methods, 2014. **67**: 205-214.

35. B. Ding, Z. Deng, H. Yan, S. Cabrini, R. Zuckermann and J. Bokor, *Gold Nanoparticle Self-Similar Chain Structure Organized by DNA Origami.* Journal of the American Chemical Society, 2010. **132**: 3248-3249.

36. P. Zhan, P. Dutta, P. Wang, G. Song, M. Dai, S. Zhao, Z. Wang, P. Yin, W. Zhang, B. Ding and Y. Ke, *Reconfigurable Three-Dimensional Gold Nanorod Plasmonic Nanostructures Organized on DNA Origami Tripod.* ACS Nano, 2017. **11**: 1172-1179.

37. D. Zanchet, C. Micheel, W. Parak, D. Gerion and A. Alivisatos, *Electrophoretic Isolation of Discrete Au Nanocrystal/DNA Conjugates.* NanoLetters, 2001. **1(1)**: 32-35.

38. S. Pal, Z. Deng, H. Wang, S. Zou, Y. Liu and H. Yan, *DNA Directed Self-Assembly of Anisotropic Plasmonic Nanostructures.* Journal of the American Chemical Society, 2011. **133(44)**: 17606-17609.

39. S. Park, A. Lazarides, J. Storhoff, L. Pesce and C. Mirkin, *The Structural Characterization of Oligonucleotide-Modified Gold Nanoparticles Networks Formed by DNA Hybridization.* J. Phys. Chem. B, 2004. **108**: 12375-12380.

40. nanoComposix. (2017). *Lateral Flow Assay Development Guide. 1.1.*

41. K. Wagenbauer, F. Engelhardt, E. Stahl, V. Hechtl, P. Stommer, F. Seebacher, L. Meregalli, P. Ketterer, T. Gerling and H. Dietz. *How we make DNA origami*. ChemBioChem.

42. E. Getz, W. Chakrabarty, R. Cooke and P. Selvin. *A Comparison between the Sulfhydryl Reductants Tris(2-carboxyethyl)phosphine and Dithiothreitol for Use in Protein Biochemistry*. Analytical Biochemistry, 1999. **273**: 73-80.

43. H. Hill, J. Millstone, M. Banholzer and C. Mirkin. *The Role Radius of Curvature Plays in Thiolated Oligonucleotide Loading on Gold Nanoparticles*. ACS Nano, 2009. **3(2)**: 418-424.

44. S. Hurst, A. Lytton-Jean, and C. Mirkin. *Maximizing DNA Loading on a Range of Gold Nanoparticle Sizes*. Analytical Chemistry, 2006. **78**: 8313-8318.

45. X. Zhang, M. Servos, J. Liu. *Instantaneous and Quantitative Functionalization of Gold Nanoparticles with Thiolated DNA Using a pH-Assisted and Surfactant-Free Route*. Journal of the American Chemical Society, 2012. 134, 7266-7269.

46. M. Srisa-Art, E. Dyson, A. deMello and J. Edel. *Monitoring of Real-Time Streptavidin-Biotin Binding Kinetics Using Droplet Microfluidics*. Analytical Chemistry, 2008. **80**: 7063-7067.

47. C. Holstein, S. Bennett, C. Anderson, K. Keniston, C. Olsen, B. Li, B. Bales, D. Moore, E. Fu, D. Baker and P. Yager. *Immobilizing affinity proteins to nitrocellulose: a toolbox for paper-based assay developers*. Analytical Bioanalytical Chemistry, 2016. **408(5)**: 1335-46.

48. N. Raston, V. Nguyen. and M. Gu, *A new lateral flow strip assay (LFSA) using a pair of aptamers for the detection of Vaspin*. Biosensors and Bioelectronics, 2017: **93**: 21-25.

49. A. Kolosova, L. Sibanda, R. Verheijen and C. Peteghem. *Development of a colloidal gold-based lateral-flow immunoassay for the rapid simultaneous detection of zearalenone and deoxynivalenol*. Anal Bioanal Chem, 2007. **389**: 2103-2107.

50. D. Chiao, C. Hu, H. Chiang and S. Tang. *Colloidal gold-based immunochromatographic assay for detection of botulinum neurotoxin type B*. Journal of Chromatography B, 2004. **809:** 37-41.

51. Zhao et al. *Paper-Based Bioassays Using Gold Nanoparticle Colorimetric Probes*. Anal. Chem., 2008. **80**: 8431-8437

52. H. Xu, X. Moa, Q. Zeng, S. Wang, A. Kawde and G. Liu. *Aptamer-Functionalized Gold Nanoparticles as Probes in a Dry-Reagent Strip Biosensor for Protein Analysis*. Anal. Chem., 2009. **81(2)**: 669-675

53. J. Tate, G. Ward. *Interferences in Immunoassay*. Clin Biochem Rev., 2004. **25(2)**: 105-120.

54. R. Jungmann, C. Steinhauer, M. Scheible, A. Kuzyk, P. Tinnefeld and F. C. Simmel. *Single-Molecule Kinetics and Super-Resolution Microscopy by Fluorescence Imaging of Transient Binding on DNA Origami.* Nano Lett., 2010. **10**: 4756-4761.

APPENDIX A: IRB Approval Letter

MARSHALL UNIVERSITY.
www.marshall.edu

Office of Research Integrity

August 28, 2018

Adrienne Walker
116 Hidden Cove
Scott Depot, WV 25560

Dear Ms. Walker:

This letter is in response to the submitted thesis abstract entitled *"A Novel DNA Origami Based Lateral Flow Assay."* After assessing the abstract, it has been deemed not to be human subject research and therefore exempt from oversight of the Marshall University Institutional Review Board (IRB). The Code of Federal Regulations (45CFR46) has set forth the criteria utilized in making this determination. Since the information in this study does not involve human subjects as defined in the above referenced instruction, it is not considered human subject research. If there are any changes to the abstract you provided then you would need to resubmit that information to the Office of Research Integrity for review and a determination.

I appreciate your willingness to submit the abstract for determination. Please feel free to contact the Office of Research Integrity if you have any questions regarding future protocols that may require IRB review.

Sincerely,

Bruce F. Day, ThD, CIP
Director

WE ARE... **MARSHALL.**
One John Marshall Drive • Huntington, West Virginia 25755 • Tel 304/696-4303
A State University of West Virginia • An Affirmative Action/Equal Opportunity Employer

80

APPENDIX B: LIST OF ABBREVIATIONS

AuNP...Gold nanoparticle

CO or CO_3970...Cross Origami 3970

CO(I)...CO immobile probe

CO(M)...CO mobile probe

TBA...Thrombin-binding aptamer

ZKV...Zika Virus

NC...Nitrocellulose

1xCOB........................Tris-acetate 40mM, EDTA 20mM, MgCl$_2$ 12.5mM – DNA Origami buffer

AFM... Atomic Force Microscopy

nM ....Molar (10^{-9})

ssDNA ....single-stranded DNA

dsDNA..double-stranded DNA

NTA ....Nitrilotriacetate

Tris-NTA...Tris-Nitrilotriacetic Acid

PBS ....Phosphate-buffered saline

BSA..Bovine serum albumin

LFA..Lateral flow assay

CFP..Cyan fluorescent His-tagged protein

hCG...Human chorionic gonadotropin

LSPR..Localized surface plasmon resonance

TCEP..Tris(-carboxyethyl)phosphine